AD-A107 321 FOREIGN TECHNOLOGY DIV WRIGHT-PATTERSON AFB OH F/G 9/5
ANTENNA (SELECTED ARTICLES),(U)
OCT 81 D N TRUSKANOV, A A PISTOL'KORS
UNCLASSIFIED FTD-ID(RS)T-0937-81 NL

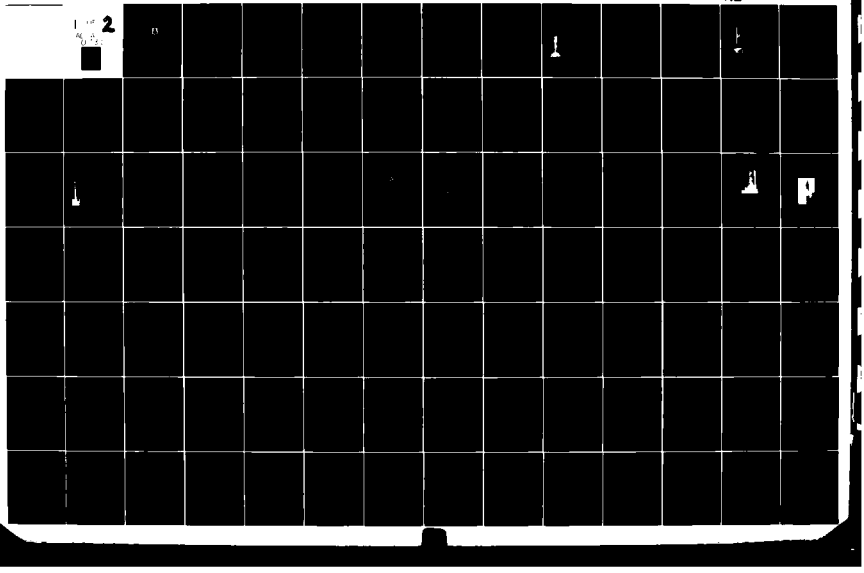

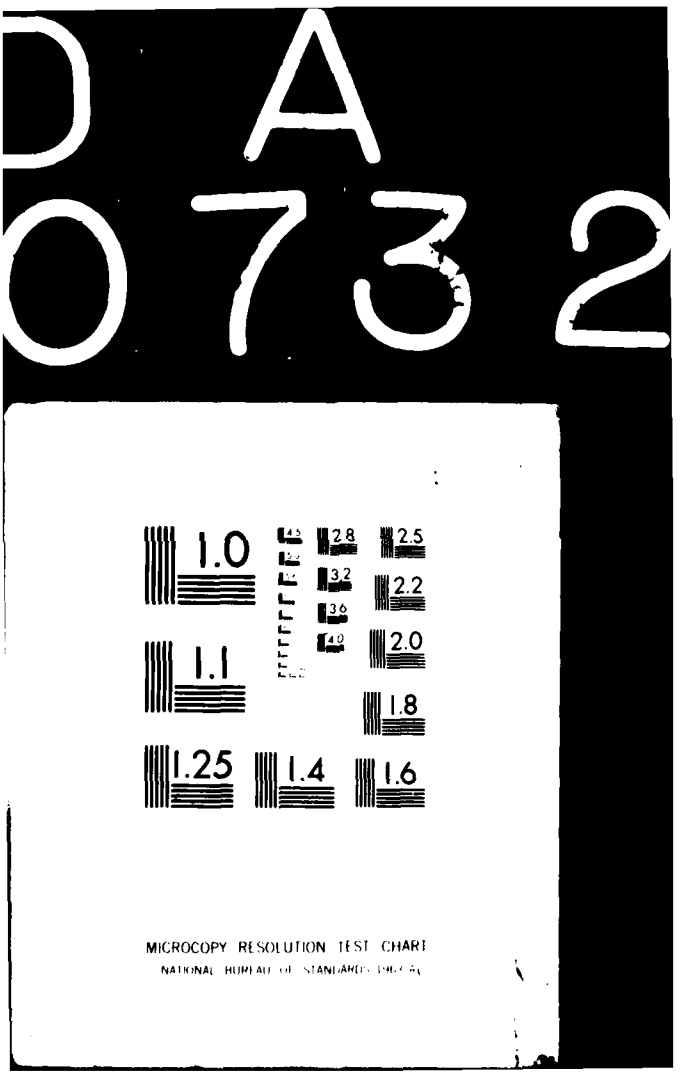
D A
0732
1.0
1.1
1.25
1.4
1.6
2.8
3.2
3.6
4.0
2.5
2.2
2.0
1.8
MICROCOPY RESOLUTION TEST CHART
NATIONAL BUREAU OF STANDARDS 1963-A

FTD-ID(RS)T-0937-81

FOREIGN TECHNOLOGY DIVISION

ANTENNA

(Selected Articles)

DTIC
ELECTE
NOV 1 8 1981
A

AD A107321

DTIC FILE COPY

Approved for public release;
distribution unlimited.

EDITED TRANSLATION

FTD-ID(RS)T-0937-81 19 October 1981

MICROFICHE NR: FTD-81-C-000963

ANTENNA (Selected Articles)

English pages: 91

Source: Antenny, Nr. 2, 1967, pp. 4-32, 55-70, 117-130, 166-178

Country of origin: (USSR)
Translated by: LEO KANNER ASSOCIATES
F33657-81-D-0264
Requester: FTD/TQFE
Approved for public release; distribution unlimited.

THIS TRANSLATION IS A RENDITION OF THE ORIGINAL FOREIGN TEXT WITHOUT ANY ANALYTICAL OR EDITORIAL COMMENT. STATEMENTS OR THEORIES ADVOCATED OR IMPLIED ARE THOSE OF THE SOURCE AND DO NOT NECESSARILY REFLECT THE POSITION OR OPINION OF THE FOREIGN TECHNOLOGY DIVISION.

PREPARED BY:

TRANSLATION DIVISION
FOREIGN TECHNOLOGY DIVISION
WP-AFB, OHIO.

TABLE OF CONTENTS

U. S. Board on Geographic Names Transliteration System..... ii

The Developmnet of Domestic Technology for Television Transmitting Antennas, by D. M. Truskanov..... 1

Discrimination of Hologram and Antenna Theory, by A. A. Pistol'kors..... 38

Radiation of an Antenna in the Form of a Ribbed Shaft of Finite Length, by G. D. Malushkov..... 58

Possibilities of Phase Correction on the Small Reflection in a Two-Reflector Antenna, by A. L. Ayzenberg..... 75

Accession For
NTIS GRA&I
DTIC TAB
Unannounced
Justification
By
Distribution/
A

U. S. BOARD ON GEOGRAPHIC NAMES TRANSLITERATION SYSTEM

Block	Italic	Transliteration	Block	Italic	Transliteration
А а	*А а*	A, a	Р р	*Р р*	R, r
Б б	*Б б*	B, b	С с	*С с*	S, s
В в	*В в*	V, v	Т т	*Т т*	T, t
Г г	*Г г*	G, g	У у	*У у*	U, u
Д д	*Д д*	D, d	Ф ф	*Ф ф*	F, f
Е е	*Е е*	Ye, ye; E, e*	Х х	*Х х*	Kh, kh
Ж ж	*Ж ж*	Zh, zh	Ц ц	*Ц ц*	Ts, ts
З з	*З з*	Z, z	Ч ч	*Ч ч*	Ch, ch
И и	*И и*	I, i	Ш ш	*Ш ш*	Sh, sh
Й й	*Й й*	Y, y	Щ щ	*Щ щ*	Shch, shch
К к	*К к*	K, k	Ъ ъ	*Ъ ъ*	"
Л л	*Л л*	L, l	Ы ы	*Ы ы*	Y, y
М м	*М м*	M, m	Ь ь	*Ь ь*	'
Н н	*Н н*	N, n	Э э	*Э э*	E, e
О о	*О о*	O, o	Ю ю	*Ю ю*	Yu, yu
П п	*П п*	P, p	Я я	*Я я*	Ya, ya

*ye initially, after vowels, and after ъ, ь; e elsewhere.
When written as ё in Russian, transliterate as yё or ё.

RUSSIAN AND ENGLISH TRIGONOMETRIC FUNCTIONS

Russian	English	Russian	English	Russian	English
sin	sin	sh	sinh	arc sh	sinh^{-1}
cos	cos	ch	cosh	arc ch	cosh^{-1}
tg	tan	th	tanh	arc th	tanh^{-1}
ctg	cot	cth	coth	arc cth	coth^{-1}
sec	sec	sch	sech	arc sch	sech^{-1}
cosec	csc	csch	csch	arc csch	csch^{-1}

Russian	English
rot	curl
lg	log

THE DEVELOPMENT OF DOMESTIC TECHNOLOGY FOR TELEVISION TRANSMITTING ANTENNAS

D. M. Truskanov

Set forth briefly in the article is the history of the development of domestic technology for television transmitting antennas and its contemporary state.

Described herein are the principles of construction of feed circuits of the antennas with repeated compensation of the reflections.

Also given are the characteristics of typical multiprogram antenna systems mounted on masts 235 and 350 m in height, as well as unique tower antenna systems 316 m in height in Leningrad, and 533 m in height in Moscow (Ostankino).

Brief Historical Synopsis

In connection with the vast expansion of the network of television broadcasting in the Soviet Union, it is of interest to trace the development of domestic technology for television transmitting antennas, which determine the quality of the transmitted image to a considerable extent.

The first studies on the creation of transmitting television antennas were begun in 1934, when, under the direction of V. V.

Tatarinov, a vertical single-tier antenna was developed, fed by a symmetrical high-resistance line. In order to improve the frequency properties, the antenna dipoles were made from tubing of larger diameter.

In the first functional domestic television station (in Leningrad), which was put into operation in 1938, a vertical single-tier antenna of tubular emitters, developed in 1936, was also utilized as a transmitting antenna. In contrast to the Tatarinov antenna, the diameter of the emitters was less, and feed was accomplished through a circuit with a shunt. It is interesting to note that, although ultrashort waves were utilized for transmission of the television image, the sound track was delivered through a medium-wave station.

During the period from 1936 through 1940, in the laboratory headed by N. S. Neyman, research studies were carried out on the study of the properties of various emitting systems, with the goal of their use during the creation of transmitting television antennas.

Carried out in 1938 were studies of V-antennas, conical dipoles, dipoles of special form with low wave resistance, fed cophasally and in quadrature with horizontal polarization, and so on. A multi-tier cophasal antenna, consisting of two mutually-perpendicular horizontal dipoles in each tier, fed with a 90° phase shift, was proposed by Ramlau and Pistol'kors as early as 1929 [1]. It was subsequently noted that such feeding substantially improves the frequency characteristic of the antenna-feeder circuit. Subsequently, antennas fed in a similar manner received widespread dissemination, and were called turnstile antennas.

Monitoring of the operating conditions of the feeder lines and antennas is important for normal operation of television antennas. In 1939, A. A. Pistol'kors proposed unidirectional

couplers for measuring the traveling wave coefficient (kbv), and somewhat later, M. S. Neyman and A. A. Pistol'kors proposed feeder reflectometers [2], based on the utilization of couplers, which make it possible to directly measure the traveling wave coefficient in the feeder. Reflectometers, studied in detail by A. R. Vol'pert in 1940-1941 [3], and directional couplers are widely utilized at the present time for monitoring the operation of antenna and feeder devices, not only in the Soviet Union, but also abroad.

Developed in 1939 was a preliminary design of a television antenna for the Palace of Soviets. During the development of this design, the problem of producing a nondirected pattern, with placement of the emitters around bodies of larger cross-sections, was first encountered. In the design process, M. S. Neyman formulated the basic requirements for transmitting television antennas, and the principles of their construction, many of which have not lost their value even at the present time [4].

With the beginning of the Great Patriotic War, studies in the area of transmitting television antennas were, in essence, halted.

Begun in the post-war years were intensive research studies on the creation of directional multi-tier broad-band antennas. At the beginning of 1946, B. V. Braude proposed a planar dipole for television antennas, which ensures a high level of matching with the feeder in a broad band of frequencies [5].

Developed in 1946-1947 under the direction of B. V. Braude, and put into operation in 1948, was a three-tier turnstile antenna for the Moscow Television Station (MTTs), designed for simultaneous operation of television and sound transmitters, using the appropriate separator filters. In being the most powerful antenna at that time, it made it possible, in view of

its broad-band nature, to considerably improve the quality of the television image. A single-tier antenna of planar dipoles was also installed at the Leningrad Television Station in 1948. It should be noted that information on similar developments abroad, particularly in the United States, appeared in the Soviet Union somewhat later.

Subsequently, in 1951, an antenna, basically similar to the antenna in the MTTs, was mounted and put into operation in Kiev (Fig. 1), with the difference that, at the feed point, the dipoles were fastened with metallic, rather than ceramic, insulators.

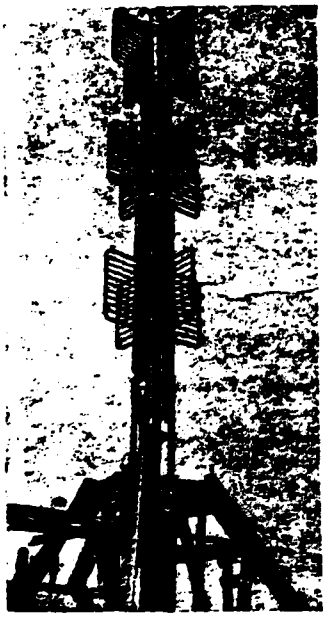

Fig. 1. Three-tier antenna of single planar dipoles.

By the beginning of the 1950's, three television stations had been placed into operation in the Soviet Union: in Moscow, Kiev, and Leningrad. These television stations were equipped with turnstile antennas with planar single dipoles. Although the antenna gain of these antennas did not exceed three, they were unique in accommodated power not only for Soviet, but also foreign technology of that time.

The subsequent years were devoted to the creation of typical designs of antennas on five frequency channels in the 48.5-100 MHz range. These studies culminated in roughly 1955 with the development of a typical design of a free-standing tower-antenna 180 m high, designed to accommodate a turnstile television antenna, and a radio station antenna for two-program ultrashort wave frequency-modulated broadcasting. The upper part of the tower was made in the form of a $1.75 \times 1.75 \times 25$ m^3 prism, around which the dipoles of the ultrashort wave frequency-modulated

broadcast antenna were placed, operating at any frequency in the 67-73 MHz range. The television antenna was mounted directly above the prism. The utilization of high frequencies, up to 100 MHz, for transmission of television programs made it possible to substantially increase the amplification of the antennas by means of the use of a larger number of tiers. Duplex planar dipoles [6], which make it possible to simplify the antenna feed system, proved more convenient for these antennas.

Given in Table 1 are the basic electrical parameters of the typical designs of turnstile television antennas developed in 1953-1954. The overall appearance of the tower with the antennas is shown in Fig. 2.

The frequency-modulated broadcasting antenna was made of six stages of cophasally-fed curved wave dipoles, located on opposite faces of the prism. The adopted configuration of the antennas was a prototype of the subsequently-developed multi-program antenna systems.

Table 1

(c) Номер канала	(d) Диапазон частот *Мгц*	(a) Мощность телевизионного и звукового передатчиков соответственно 5 и 2,5 *квт*			(b) Мощность телевизионного и звукового передатчиков соответственно 15 и 7,5 *квт*		
		(e) число этажей сдвоенных вибраторов	(f) усиление по сравнению с изотропн. излучателями	(g) ков в диапазоне частот	(e) число этажей сдвоенных вибраторов	(f) усиление по сравнению с изотропным излучателем	(g) ков в диапазоне частот
1	48÷56	2	3,6	0,85	2	3,6	0,85
2	58÷66	2	3,6	0,85	2	3,6	0,85
3	76÷84	3	5,6	0,85	3	5,6	0,85
4	84÷92	4	7,2	0,85	3	5,6	0,85
5	92÷100	4	7,2	0,85	3	5,6	0,85

Key: (a) Power of television and sound transmitters, respectively, of 5 and 2.5 kW; (b) Power of television and sound transmitters, respectively, of 15 and 7.5 kW; (c) Channel number; (d) Range of frequencies, MHz; (e) number of stages of duplex dipoles; (f) amplification, as compared with isotropic emitters; (g) traveling wave coefficient in frequency range.

Also developed, simultaneously with the antennas, were separator filters for combined operation of television and sound transmitters on a single antenna, which create bypassing at 25-30 db.

Contemporary State of Technology of Transmitting Television Antennas

General Information. The sharp increase in the number of constructed television stations in our country, the utilization for these purposes of a very broad range of frequencies (48-100 MHz, 174-230 MHz, 470-622 MHz) and the switch to multiprogram television broadcasting posed new problems for antenna technology. Two basic problems appeared here, the solution of which proved decisive during the creation of modern television antennas. These include the problem of the so-called "feeder echo" and the problem of creation of radiation patterns, not directed in the horizontal plane and approaching a "cosecant" form in the vertical plane.

The Battle Against "Feeder Echo". As was already indicated, in 1939, M. S. Neyman formulated the basic principles and problems of the construction of television transmitting antennas. Here, the phenomenon of "feeder echo" was first predicted, as a result of which so-called multiple images occur at the receiving end of the radio line.

From the point of view of transmitting antennas, the cause of the appearance of multiple images on the television screen is nonideal matching of the antenna with its supply feeder. With poor matching, part of the energy radiates into space, and part, the magnitude of which is determined by the degree of mismatching, is reflected towards the transmitter, and then, after reflection from it, passing along a path equal to twice the length of the feeder, is again radiated, reaching the receiving antenna with a time lag in the form of a multiple image. The struggle against

the phenomenon of "echo" may principally be carried out in several ways:

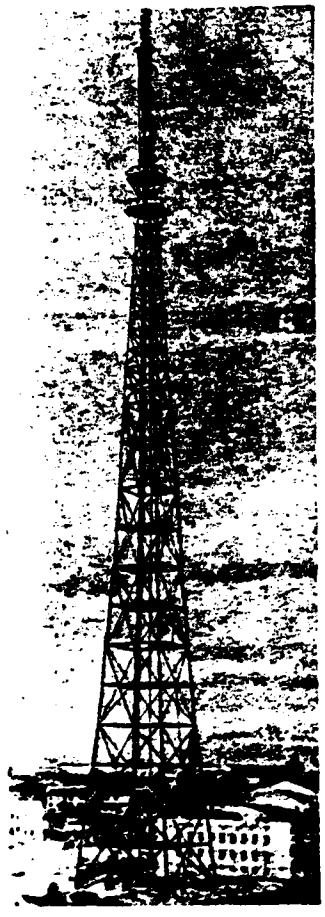

Fig. 2. Typical tower, 180 m high, with a three-tier television antenna of duplex dipoles and an antenna for kilowatt-hour frequency-modulated broadcasting.

- direct improvement of the frequency properties of the transmitting antennas in order to reduce reflections and, consequently, the intensity of the multiple circuits to magnitudes which lie beyond the limits of discernibleness of the eye;

- reduction of the reflection coefficient of the transmitting device for electromagnetic waves, traveling on the side of the antenna;

- the creation and radiation on the transmitting end of the radio line, along with the basic signal, of an auxiliary lag signal, the intensity of which should correspond to the intensity of the "feeder echo" signal, but with reverse polarity.

As a result of studies on the first of the indicated trends, feed schematics were proposed for antennas with repeated compensation of the reflections, a detailed description of which will be given below [7], [8].

A decrease in the coefficient of reflection on the transmitting end of the radio line was achieved using a power equalizer, the schematic of which for transmitting devices was proposed by E. S. Glazman [9]. The use of such an equalizer makes it possible to almost completely absorb the

energy reflected from the transmitting antenna, and thereby prevent the appearance of substantial multiple images.

Studies of the third means of creation of an auxiliary signal with polarity inverse to the "feeder echo" did not provide completely satisfactory results, as a result of which this method did not receive dissemination.

Production of the Required Radiation Patterns. For the vast territory of the Soviet Union, the basic type of beam pattern is, naturally, the nondirectional pattern. However, the creation of such a pattern with slight irregularity is associated with a number of difficulties, especially during the construction of multi-tier antennas.

The form of the beam pattern of the antenna in the horizontal plane depends on the separation between the emitters —with an increase in the separation, the irregularity of the pattern increases. During the creation of multi-tier turnstile antennas, this circumstance limited the diameter of the central carrier conduit, and consequently, according to the conditions of the required rigidity with regard for wind, also the number of tiers and the amplification of the antenna.

The use of methods of inter-tier compensation for turnstile antennas made it possible to substantially reduce the irregularity of the pattern, or, all other things being equal, to increase the permissible diameter of the carrier conduit, and, consequently, the height of the antenna.

With the switch to multiprogram antenna systems, where the antennas are located one above the other, the cross-section of the carrier constructions increases sharply. In this case, the nondirectional pattern may be produced through utilization of a larger number of emitters, located around the support, as was designed, for example, for the Palace of Soviets in 1939.

However, an increase in the number of dipoles, and, consequently, complication of the feeder supply system, leads to a considerable rise in price of both the antennas themselves, and of the tower, since the weight and wind load increase simultaneously.

Thus, in the given case, the problem amounts not simply to the production of a sufficiently uniform pattern, but to the production of its most economical systems, i.e., with the minimal number of emitters in a tier.

As a result of the conduct of lengthy and quite time-consuming theoretical and experimental studies, it was established that, in the majority of cases, one must utilize four emitters in a tier to produce a sufficiently uniform pattern. In this case, it was revealed that the use of variable-phase feed of the emitters is possible only on supports with a cross-section which does not exceed $(0.8\text{-}1)\lambda$. At the same time, with cophasal feed of the tier emitters, supports are possible with a cross-section of up tc $(1.8\text{-}2)\lambda$.

Thus, from the point of view of the utilization of supports of greater cross-section, a cophasal system is preferable in some cases. However, it lags considerably behind a variable-phase system in its frequency properties.

The use of a schematic of multiple inter-tier compensation for the case of cophasal emitter feed inside the tier makes it possible to combine the advantages of both systems.

Simultaneously with an increase in the amplification of the antenna, the radiation pattern narrows down in the vertical plane, and the number of side lobes increases simultaneously. All of this leads to expansion of the zones of distorted receiving, and an increase in their number. In order to prevent this, special measures for the creation of lobeless beam patterns of a special

form of the "cosecant" type are envisaged with the utilization of multi-tier antennas. Such a form of the pattern is usually combined with a slight inclination of the main lobe in the direction of the horizon for the best utilization of the power radiated by the antenna [4].

Principles of Construction of Antenna Feed Schematics with Multiple Reflection Compensation

Previously, during the development of television antennas, one usually proceeded from the necessity of development of the emitting elements of the antennas so that the traveling wave coefficient in the supply feeder lay within limits which ensure the absence of a substantial repeated outline on the image. In this case, it was considered successful to obtain a traveling wave coefficient equal to 0.8-0.85 in the band of only a single or several television channels. With carrying out of research studies in the last decade, a different approach was selected, namely: relatively low requirements were placed on the emitters, and, at the same time, requirements more rigid than before were placed on matching of the entire set of emitters, associated with the feeder supply system.

As was already noted, during the study of turnstile antennas of two mutually-perpendicular dipoles, it was noted as early as the 1930's that their feed with phase shift of 90° improves the traveling wave coefficient in the frequency band. In this case, the reactances are partially compensated, and the resistances approach a magnitude of W/2. The varieties of the known feed schematics of turnstile television antennas, used both in the Soviet Union and abroad, as well as their equivalent schematics, are given in Fig. 3. For proper operation of the antenna (Fig. 3a, b), the voltages and currents in the dipoles 2-4 should be shifted in phase relative to the currents and voltages in the dipoles 1-3 by 90°. In addition, there should be a phase shift by 180° between the voltages on the dipoles 1 and 3 and 2 and 4.

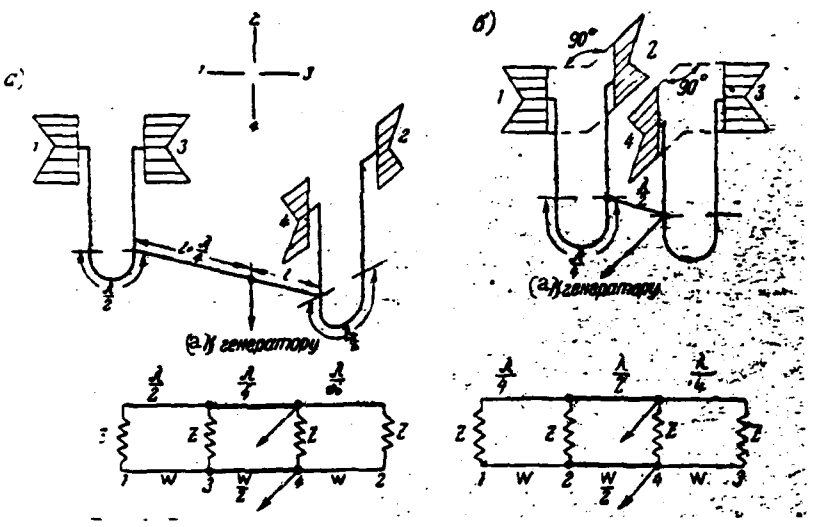

Fig. 3. Various feed schematics of turnstile television antennas.
Key: (a) to generator.

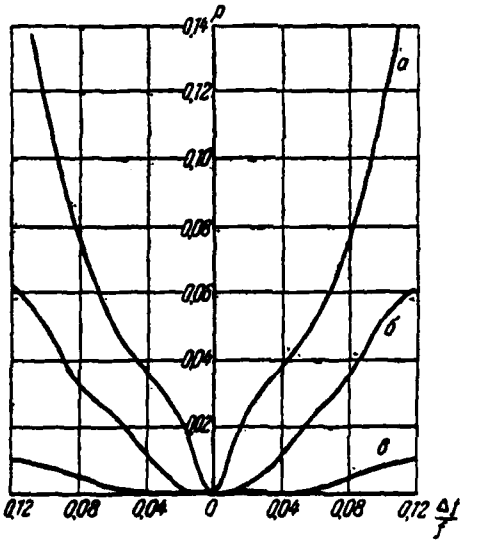

Fig. 4. Coefficient of reflection of single-tier antenna: a - according to schematic in Fig. 3a; b - according to the schematic in Fig. 3b; c - with double compensation according to the schematic in Figs. 5 and 6.

The coefficient of reflection for these systems,

calculated on the assumption that the input conductivity of the emitters changes in the frequency range ±12% from 1 to 0.7 is shown in Fig. 4. If four dipoles (or half-dipoles), each of which differs in phase from the adjacent dipole by 90°, are located in a single tier of the antenna, their feed schematic may be constructed so that compensation of the reflections will occur twice (Figs. 5 and 6).

Actually, if the dipoles are fed in pairs with a 90° shift, then at the point of their inclusion, there occurs the first stage of compensation. It is easy to see that the combining of the two groups (of two dipoles each) with a 90° shift will provide the second stage of compensation at the point of their inclusion, and, consequently, further improvement of matching with the supply feeder. In this case, the phasing required for proper operation of the antenna is assured by "crossed" feed of one of the dipoles (Fig. 5). The coefficient of reflection for this schematic is given in Fig. 4.

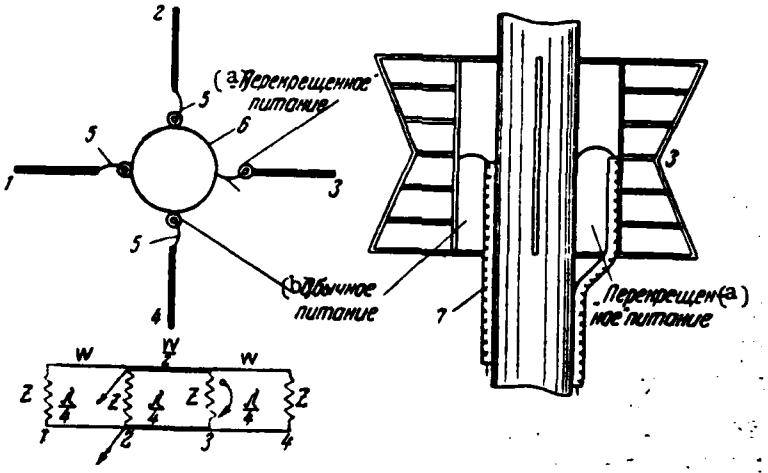

Fig. 5. Feed of one tier of a turnstile antenna according to a schematic with two-fold compensation: 1, 2, 3, 4 - dipoles, 5 - connectors, 6 - carrier conduit, 7 - cable. Key: (a) "crossed" feed; (b) normal feed.

During the construction of multi-tier antennas, this principle may be utilized both within the limits of each tier, and with

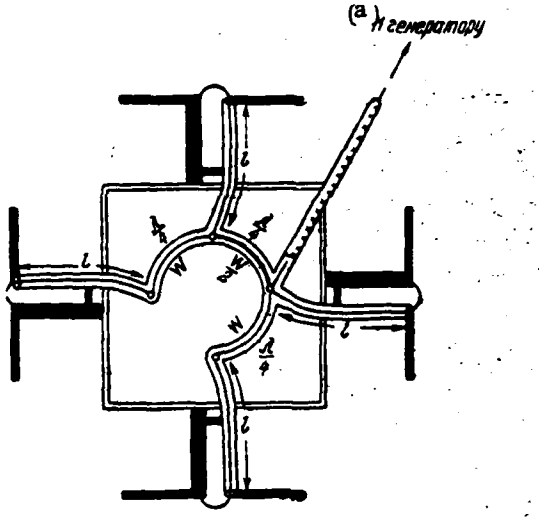

Fig. 6. Feed of one tier of a circular antenna with two-fold compensation.
Key: (а) to the generator.

interconnection of the tiers. It is easy to see that, if each of the stages is implemented according to a schematic with quadrature feed, then, with feeding of two tiers which are not in phase, as usual, and with 90° shift, one more stage of compensation appears at the point of their connection. In this case, for a cophasal composition of the fields created by the tiers, one of them rotates in an appropriate manner by 90° in space (Fig. 7). In the figure, the dipoles with a single number are located one above the other, and the circular arrow denotes "crossed feed". In case of necessity, the next stage of compensation may be achieved through joining of the groups of tiers, and so on. Such compensation received the name "inter-tier". As was already stated, in this case, the beam pattern improves substantially in the horizontal plane (Fig. 8).

It goes without saying that multiple compensation is also possible with feed of an antenna with a different number of emitters in a tier. In this case, with parallel connection of n emitters, their supply feeder lines should differ in length by

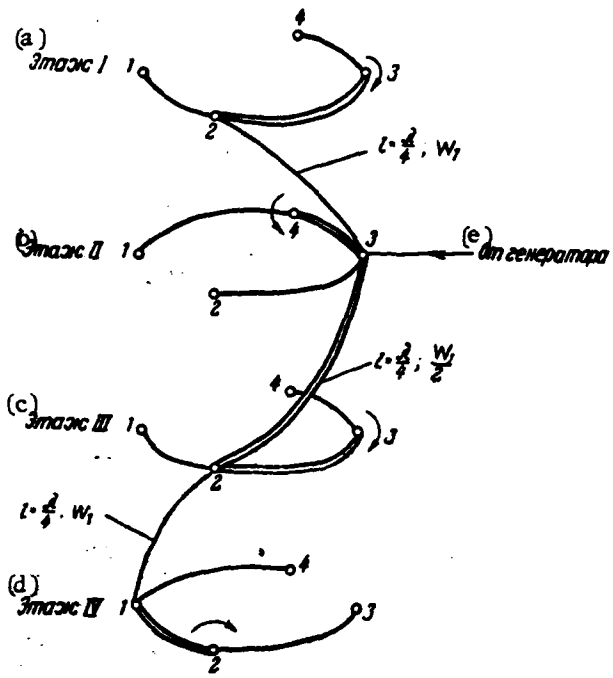

Fig. 7. Feed of four-tier antenna according to a schematic with four-fold compensation. Key: (a) tier I; (b) tier II; (c) tier III; (d) tier IV; (e) from generator.

$2\pi/n$ rad from one another. It should, however, be noted that such compensation will be effective only with the absence of a mutual effect among the emitters.

Under some conditions, the described principle may also be utilized during the construction of multi-tier antennas with cophasal feed in the tier (see below). All that has been said applies to both turnstile and circular antennas.

It is advisable to examine the schematic in Fig. 9 for the study of the behavior of schematics with multiple compensation of the reflections with operation in a broad range of frequencies. Assuming that the traveling wave coefficient in the connected lines is equal to k, the summary dimensionless conductivity of the entire system may be written as:

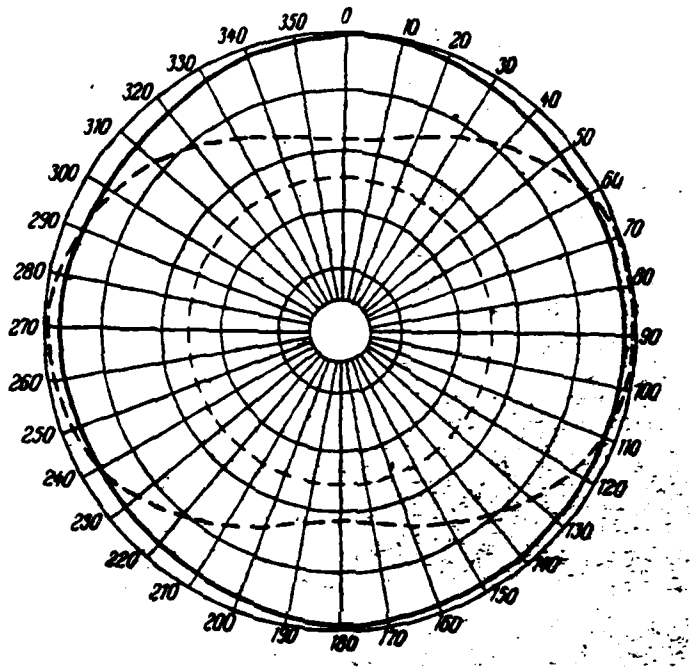

Fig. 8. Beam pattern of two-tier turnstile antenna in the horizontal plane (dotted line - pattern with normal feed schematic, solid line - with feed with inter-tier compensation).

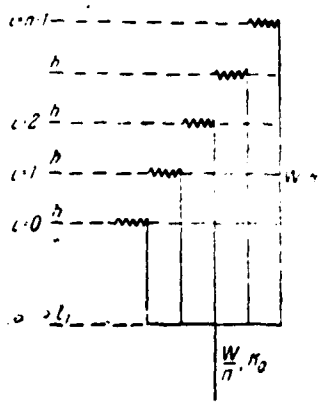

Fig. 9. Schematic of parallel connection of loads.

$$y_n \approx \frac{1}{n} \sum_{i=0}^{i=n-1} \frac{k + i(1 - k^2)^2 \sin ih \cos ih}{\cos^2 ih + k^2 \sin^2 ih}. \qquad (1)$$

Here, h is the difference in feeder lengths, rad,

n is the number of emitters,

i is the ordinal reference number, with i=0 at the first emitter.

For simplificiation of analysis of expression (1) with random values of h and n, we will use Euler's formula, which expresses the relationship between the

sum and the integral [10].

Introducing the designations

$$f(x)=\frac{k+i(1-k^2)\sin x\cos x}{\cos^2 x+k^2\sin^2 x} \tag{2}$$

and

$$nh=x_0, \tag{3}$$

we have

$$y_n=\frac{1}{x_0}\int_0^{x_0}f(x)dx-\frac{1}{2n}[f(x_0)-f(0)]+\frac{x_0}{12n^2}[f'(x_0)-f'(0)]-$$
$$-\frac{x_0^3}{720n^4}[f'''(x_0)-f'''(0)]+\ldots+(-1)^{p-1}\frac{B_p x_0^{2p-1}}{(2p)!\,n^{2p}}\times$$
$$\times\left[f^{2p-1}(x_0)-f^{2p-1}(0)\right]+R_{2p}, \tag{4}$$

$$R_{2p}=(-1)^{p+1}\frac{x_0^{2p+1}}{n^{2p}}\int_0^{x_0}f^{2p+1}(x)\left[\sum_{m=1}^{\infty}\frac{\sin 2mpx}{2^{2p}\pi^{2p+1}m^{2p+1}}\right]dx. \tag{5}$$

We will now assume that the number n is so great that, with sufficient accuracy, one may limit oneself to the integral portion of equation (4) during the calculation. Utilizing the expression f(x), we obtain the following from formula (2) after integration

$$y_n=\frac{\operatorname{arc\,tg}(k\operatorname{tg}x_0)}{x_0}+i\frac{1}{2x_0}\ln\frac{1}{\cos^2 x_0+k^2\sin^2 x_0}. \tag{6}$$

Expression (6) indicates the possibility of obtaining a high level of matching even with small values of k, only if the value of x_0 is sufficiently great in this case. Practically, this means that, if the total length of the system, which is proportional to the magnitude of x_0, is great as compared with λ, and the sizes of the steps $h=x_0/n$ are small as compared with λ, then the entire system proves to be matched in a broad range of waves. Shown in Fig. 10 is the function $y_n=f(x_0)$ for several values of k, calculated according to formula (6). As is evident from these graphs, the greatest degree of mismatching occurs with a system length which is divisible by an odd number of quarter

waves. With a system length divisible by a whole number of half-waves, matching proves to be ideal (y_n=1), with an accuracy of up to the remainder R_{2p} of expression (5). If one prescribes

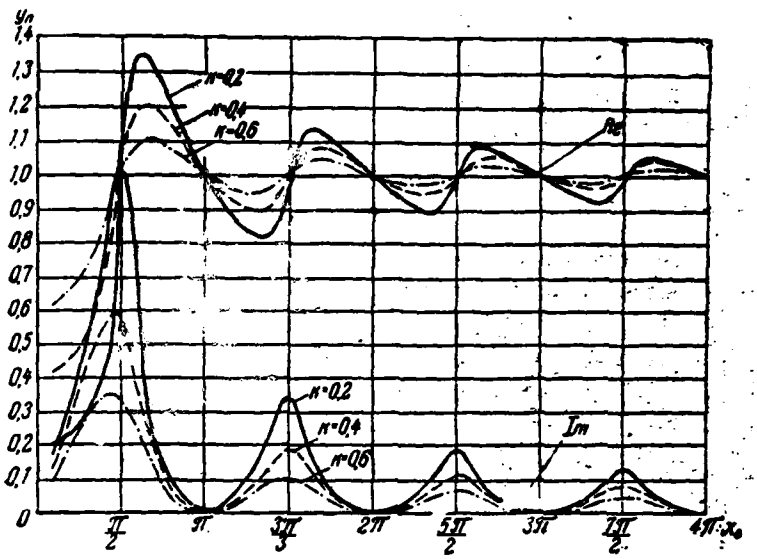

Fig. 10. Input conductivity of a system of n parallel connected loads according to the schematic in Fig. 9.

the minimal value of the traveling wave coefficient at the input of the system as equal to K_0 with values of the traveling wave coefficient in the feeder lines which form the system—k, then the minimum system length required for this, with a large number n, is determined from the inequality

$$x_0 \geqslant \frac{1}{1-K_0} \ln \frac{1}{k}. \qquad (7)$$

With calculations according to formula (7), one should bear in mind that $1-K_0$ assumes a magnitude which is small as compared with one. Thus, for example, if it is necessary to obtain a value of K_0 of no less than 0.95, with a value of k in the feeders which form the system, equal to 0.5, then the total length of the system should be at least 2.2 λ. Calculation of the magnitude of the maximum permissible dimensions of the individual steps proves most complex for the case when the total length of the

system x_0 is divisible by a whole number of half-waves, since, in this case, all of the additional terms in equation (5) prove to be equal to zero, and the difference between the sum and the integral is determined only by the remainder. For this specific case, a result may be obtained by direct summation of the series (1).

In place of the traveling wave coefficients, we will introduce the coefficients of reflections, which correspond to them, according to the known formulas:

$$p = \frac{1-k}{1+k}; \quad p_0 = \frac{1-y_n}{1+y_n}; \quad K_0 = \frac{1-|p_0|}{1+|p_0|}. \tag{8}$$

Now, let $nh=x_0=m\pi$, where m is any whole number. Then, summation of the series (1), with regard for formula (8), with m and n even, gives

$$p_0 = p^{\frac{n}{m}}, \tag{9}$$

for all other whole numbers m and n

$$p_0 = p^n. \tag{10}$$

The values of K_0 are easily determined from formula (8). The results of calculations for the case m=1 and random n are given in Fig. 11. Using schematics of quadrature compensation

$$p_0 = p^{2n}. \tag{11}$$

Here, n should be understood to mean the number of tiers of quadrature compensation.

The formulas and graphs given in the present section are correct for both parallel and series-connected feed lines. In

the latter case, it is only necessary that the wave resistance of the main feeder be n times greater than the wave resistance of the branching lines.

The principles set forth here provided the basis for the practical utilization of a number of television transmitting antennas. Actually, if one needs to implement a multiphase antenna, upon which strict requirements are placed with respect to matching in a broad band of frequencies, then the implementation of the feed system in the form of series, parallel or series-parallel schematics, in accordance with the principles set forth, makes it possible to avoid the necessity of precise matching of the emitters with their supply feeders, and, in this case, to obtain a high level of output parameters[1]. Specifically, the use

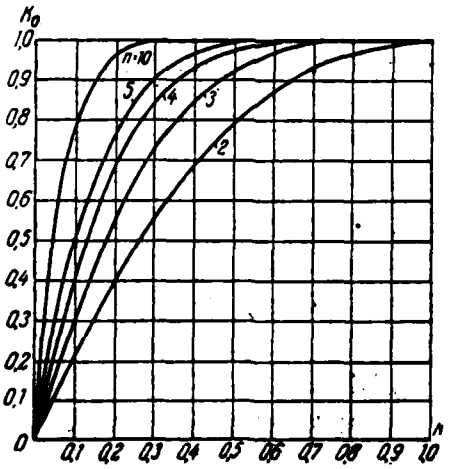

Fig. 11. Dependence of the traveling wave coefficient of the system on the traveling wave coefficient of the emitters with m=1.

[1]The principles set forth may also be used for the implementation of load equivalents, which makes it possible to substantially simplify their manufacture and adjustment.

of methods of multiple compensation for turnstile antennas made it possible to utilize a total of three types of antennas for 12 frequency channels. The parameters of the unified turnstile television antennas for radio stations with a power of 5/2.5, 15/7.5 and 5/1.5 kW are given in Table 2. Next, we will give a description of multiprogram antenna complexes, constructed utilizing the principles of multiple compensation of reflections examined above.

Table 2

(a) Номер канала	(b) Диапазон частот, *Мгц*	(c) Число этажей сдвоенных вибраторов	(d) Усиление по сравнению с изотропным излучателем на средней частоте диапазона	(e) $K_{бв}$ в диапазоне частот
1—2	48÷66	2	3,6	0,9
3—5	76÷100	4	7,2	0,9
6—12	174÷230	8	11,2	0,9

Key: (a) channel number; (b) frequency range, MHz; (c) number of tiers of duplex dipoles; (d) amplification as compared with an isotropic emitter at the average frequency of the range; (e) traveling wave coefficient in frequency range.

Antenna Systems for Multiprogram Television Stations

General Information. With the creation of multiprogram antenna complexes utilizing a single support, the antennas are located one above the other, with the height of the antenna portion, as a function of the number of programs and the utilized ranges, comprising 100-150 m. At the same time, the total height of the tower or mast facility reaches several hundred meters.

Naturally, the cross-section of the supports must be selected not only for electrical reasons, but, chiefly, from considerations of ensuring the required strength and rigidity with the effect of a wind load. With bending of the antenna structure under the influence of wind, the radiation pattern slants, and, in this case, quite considerable variations in the magnitude of the signal

at the receiving point are possible. This phenomenon is displayed more strongly the higher the antenna support and the greater the coefficient of amplification of the antenna (the narrower its beam pattern).

At the same time, the assimilation of ranges right up to 700 MHz for television leads to the necessity of an increase in the amplification of the antennas, since the conditions of propagation of radiowaves within cities, as well as the receiving conditions at these frequencies, are less favorable. On the other hand, narrowing of the beam pattern leads to a considerable increase in the number of lobes, and, consequently, also to expansion of the zone of possible distortions of the signal upon receiving. In order to eliminate such phenomena, as was already indicated, measures should be taken in the antenna which ensure filling of the gaps in the radiation between the lobes, and thus liquidation of zones of distorted receiving. With the creation of single-program antennas, mounted on typical supports (up to 180 m), and with the utilization of relatively low frequencies (up to 230 MHz), this problem did not have an acute nature, since zones of distorted receiving proved to be quite small, and were primarily located close to the television station.

One of the most important questions in the creation of multiprogram antenna complexes is the selection of the cross-section of the supports. It should be noted that the dimensions of the cross-section of the support, selected for mechanical considerations, as a rule, preclude the possibility of construction of any of the antennas according to the turnstile type. In this case, the most advisable solution is a circular antenna, in which the emitters are located around the support. On the other hand, the greater the cross-section of the support, the greater the irregularity of the radiation pattern in the horizontal plane (with a given number of emitters in a tier). At the same time, the cross-section of the support should be sufficient for the placement of the supply feeder systems of the antennas, the main

feeders, elevators, ladders, and so on, as well as to ensure convenience of maintenance and required preventive maintenance.

It is quite evident that these requirements are contradictory, and their satisfaction is possible only as a definite compromise. With the location of television stations directly in the boundaries of a city, free-standing towers are normally utilized as supports. The antenna portion of the tower is made in the form of a lattice-work prism of square cross-section with a decreasing side in proportion to the switch to the antennas located above. In this case, the antennas of the low-frequency channels are located at the bottom. The side of the cross-section of the prisms, as a function of the design and schematic of the antenna, is (0.5-1.4) λ.

With the location of television stations beyond the boundaries of a city, mast structures are more frequently utilized, which are composed of tetrahedral prismatic elements, and are fastened by several tiers of guide wires.

At the present time in the Soviet Union, there is a functional multiprogram antenna complex in Leningrad, and construction of the new Moscow complex is being completed. In addition, a typical multiprogram antenna complex is being developed for mast supports. Given below is a brief description of these systems.

The antenna complex of the Leningrad Television Station[1] makes it possible to accomplish broadcasting with three television (channels 1, 3, and 8) and three ultrashort wave frequency-modulated programs. The support tower, upon which the antenna complex is mounted, is a truncated hexahedral structure with a base equal to 60 m. The tower elements are made of steel tubing. Because of the use of high-quality grades of steel and the welded design, the total weight of the tower, together with the antenna

[1]This was covered in detail by Rushchuk, Brunin, Ivanov and other authors at the 20th All-Union Scientific Session, devoted to Radio Day in 1964.

equipment, is relatively small (about 1300 tons). The relative flexure of the body of the tower in any section does not exceed 0.01 with a maximum wind load.

The total height of the tower with the antennas is 316 m, of which 116 m are occupied by the antennas (Fig. 12), located in the following order: the lower antenna is mounted on a prism with a 6×6 m^2 cross-section, and is intended for ultrashort wave frequency-modulated broadcasting, then follows the channel 1 antenna on a 3.5×3.5 m^2 prism and the channel 3 antenna on a 2.3×2.3 m^2 prism, above which is mounted the eight-tier turnstile channel 8 antenna on a tubular base 245 mm in diameter.

The side of the prism of the frequency-modulated broadcast antenna, which is the carrier antenna for the three television antennas located above, was determined from mechancial considerations.

As the calculation showed, with this cross-section with a 1.4 λ side, the use of half-wave emitters is inadvisable, since the irregularity of the radiation characteristic in the horizontal plane exceeds the permissible norms. For this reason, wave dipoles with a cophasal feed schematic were used. The antenna has eight tiers of dipoles, with a distance of 0.75 λ between the tiers.

The channel 1 and 3 antennas are mounted on prisms, the side of which is 0.7 λ of the corresponding television channel. This fact made it possible to implement these antennas identically both in design and in electrical schematic.

In contrast to the frequency-modulated broadcast antenna, here, it proved advisable to use half-wave dipoles with quadrature feed, according to a schematic with multiple compensation. The antenna includes eight tiers of dipoles, the distance between which is equal to 0.75 λ. The feed schematic of the channel 1 and 3 antennas is given in Fig. 13. The lengths of the sections of the

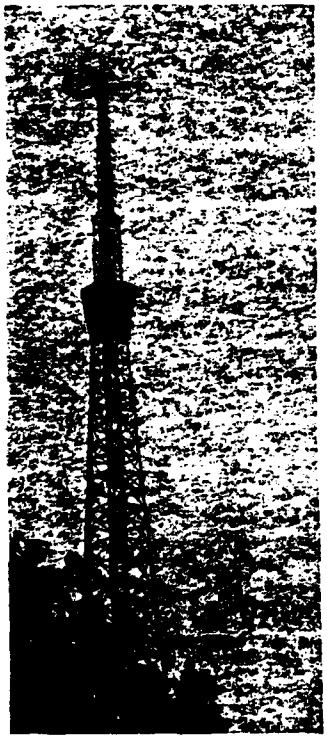

Fig. 12. General appearance of antenna complex of the Leningrad Television Station.

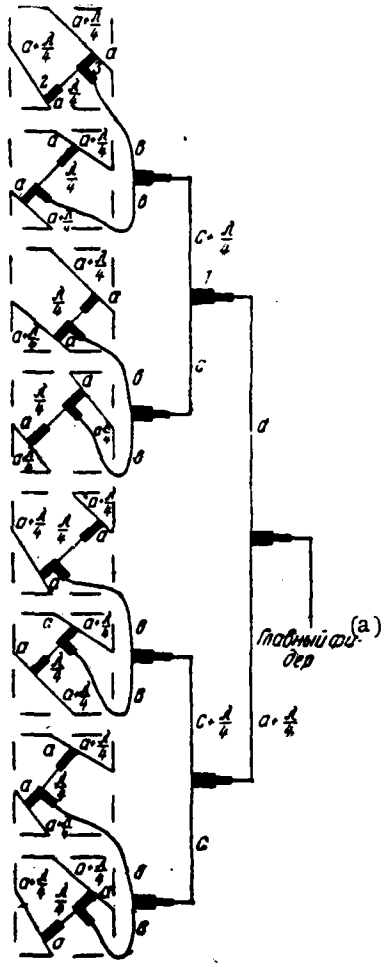

Fig. 13. Feed schematic of channel 1 and 3 television antennas.
Key: (a) main feeder.

feed cables of adjacent dipoles differ by one-fourth of the average wave length, which is ensured by quadrature feed. The second stage of compensation is achieved by the introduction of 90° phase shift between pairs of adjacent dipoles. Then, two more stages of compensation are introduced in the schematic:

between pairs of adjacent tiers and at the input of the feed system between the four-tier groups of dipoles. Such a schematic made it possible to achieve good matching of the antenna with the supply feeder (traveling wave coefficient equal to 0.94), with a sufficiently uniform horizontal radiation characteristic (±2 db).

The channel 8 antenna is an eight-tier turnstile of duplex planar dipoles, fed according to a schematic with two-fold compensation of the reflections. The coefficient of reflection at this antenna does not exceed 0.04 (traveling wave coefficient equal to 0.92).

The basic parameters of the antenna complex of the Leningrad Television Station, put into operation in 1962, are given in Table 3.

Table 3

(a) Номер канала	(c) Мощность кВт (изображение / звук)	(d) Число этажей	(e) Усиление по сравнению с изотропным излучателем	(f) Тип излучателя	(k) Кбв антенны	(l) Примечание
1	50/15	8	10	(g) конич. полуволн.	0,9	(m) Антенна панельного типа с использованием в качестве экрана конструкций опоры
3	50/15	8	10	(h) то же	0,9	
8	50/15	8	14,4	(i) сдвоенные плоскостные	0,9	(n) Антенна турникетная
(b) I-V диапазон	3×15[1])	8	10	(j) волновые вибраторы	0,7	(o) Антенна панельная

[1]Considered here is simultaneous operation with three transmitters of 15 kW each.

Key: (a) channel number; (b) frequency-modulated range; (c) power, kW (image/sound); (d) number of tiers; (e) amplification as compared with isotropic emitter; (f) type of emitter; (g) conical half-wave; (h) same; (i) duplex planar; (j) wave dipoles; (k) traveling wave coefficient of antenna; (l) note; (m) antenna of the panel type utilizing the support structures as a screen; (n) turnstile antenna; (o) panel antenna.

Table 4.

(a)												
Общая высота мачты, *м*	235						350					
(b) Общая протяженность комплекса антенн, *м*	117						150					
(c) Количество антенн	4						4					
(d) Комбинация комплекса антенн	1. (j) I диап. (l) III диап. (m) IV диап. (n) УКВ ЧМ		2 (k) II диап. (l) III диап. (m) IV диап. (n) УКВ ЧМ		3. (l) III диап. (m) IV диап. (n) УКВ ЧМ		1. (j) I диап. (l) III диап. (m) IV диап. (n) УКВ ЧМ		2 (k) II диап. (l) III диап. (m) IV диап. (n) УКВ ЧМ		3 (l) III диап. (m) IV диап. (n) УКВ ЧМ	
(e) Тип антенны	(j) I диап.	(k) II диап.	(l) III диап.	(m) IV диап.	(n) УКВ ЧМ (o) 2-прогр.	(n) УКВ ЧМ (p) 4-прогр.	(j) I диап.	(k) II диап.	(l) III диап.	(m) IV диап.	(n) УКВ ЧМ (o) 2-прогр.	(n) УКВ ЧМ (p) 4-прогр.
(f) Коэффиц. усиления по сравнению с полуволновым вибратором	6	9,5	14	25÷30	6	3	9,5	14	14	25÷30	6	3[1])
(g) Число этажей	10	18	24	50	8	4	16	24	24	50	8	4[1])
(h) Сечение опоры, *мм*^{2}	2500×2500			700××700	2500×2500		2500×2500			700××700	2500×2500	
(i) Тип передатчика и мощность, *квт*	(q) «Якорь» 5/1,5		(r) «Игла» 5/1,5	(s) «Ладога» 25/5	(t) «Дождь-2» 4+4 (u) «Дождь-3» 4+4+4+4		(v) «Ураган» 50/15		(w) «Лен» 50/15	(s) «Ладога» 25/5	(t) «Дождь-2» 4+4 (u) «Дождь-3» 4+4+4+4	

[1]) With the use of a special 4-program separating filter, the two antennas are included in parallel, and the coefficient of amplification is six.

Key: (a) Total height of mast, m; (b) Total extent of antenna complex, m; (c) Number of antennas; (d) Combination of antenna complex; (e) Type of antenna; (f) Coefficient of amplification as compared with half-wave dipole; (g) Number of tiers; (h) Cross-section of support, mm^2; (i) Type of transmitter and power, kW; (j) range I; (k) range II; (l) range III; (m) range IV; (n) ultrashort wave frequency-modulated; (o) 2-program; (p) 4-program; (q) "Anchor"; (r) "Needle"; (s) "Ladoga"; (t) "Rain-2"; (u) "Rain-3"; (v) "Hurricane"; (w) "Flax".

Typical Multiprogram Antenna Systems. The developed typical multiprogram antenna systems represent two different complexes, mounted on supports 235 and 350 m high, and intended for the basic mass of television stations and the largest regional and republic stations, respectively. The basic characteristics of the complexes and the individual antennas are given in Table 4.

The emitting elements in this type of an antenna system are symmetrical wave or half-wave dipoles, which are laid out together with the reflecting screen and fastened in parallel to the faces of the support prism. Both variable-phase and cophasal feed in the tier may be utilized for producing a nondirectional pattern.

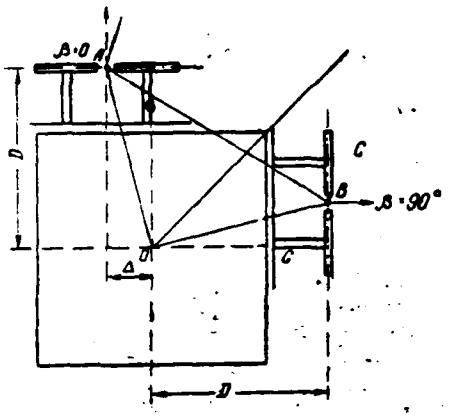

Fig. 14. Circular antenna with tangential shift of emitters.

Cophasal feed provides the least irregularity of the pattern in the horizontal plane (with large cross-sections), while variable-phase feed provides the best frequency characteristic (matching). In order to improve the pattern with variable-phase feed, so-called tangential shift of the panels is also used (Fig. 14). The emitters of two faces are not shown in the figure. In this case, the pattern of the antenna in the horizontal plane is improved (Fig. 15), as compared with the antenna without tangential shift (Figs. 16 and 17).

Antennas of television and frequency-modulated broadcasting ranges I and II of multiprogram complexes are made with tangential shift of the emitting panels, with the simultaneous use of inter-tier compensation, which ensured a traveling wave coefficient ≥ 0.9

throughout the range[1].

However, with the creation of antennas of television ranges III and IV, it proved (with the given cross-section of the support of 2.5 X 2.5 m^2) impossible to use a schematic with quadrature feed of the tier and tangential shift of the emitting elements. The fact of the matter is that, with cross-sections with a side of (1.5-1.7 λ), equalizing of the phases of the signals of adjacent emitters in the direction of the diagonal by means of their tangential shifting (Fig. 14), as is done in antennas of ranges I and II, is possible only in a narrow band of frequencies. As a result of the large separation of the dipoles, the change in the phases of the signals of the tangentially shifted emitters in the frequency range takes place within large limits, which leads to considerable irregularity of the radiation pattern on side frequencies. With such cross-sections of the supports, the obtaining of horizontal characteristics with small irregularity is possible only with a cophasal feed schematic of the emitters. In this case, the absence of 90° phase shifts between emitters does not make it possible to compensate the reflections which occur because of inaccuracy of matching. However, compensation of the reflections is all the more possible because of the inter-tier phase shifts. This is most complete if the magnitude of the phase shifts is selected as equal to π/n, where n is the number of tiers in the antenna. In this case, in the case of placement of a vertical row of emitters parallel to the axis of the support prism, the phase front, and, consequently, the main lobe of the pattern in the vertical plane, deviates from the perpendicular to the axis of the support by an angle ϕ, determined by the relationship of the wave length, the number of tiers and the distance between the tiers (Fig. 18).

[1]Antennas, produced by foreign firms, have similar parameters. In recent years in the Federated Republic of Germany, they have also begun to use schematics of inter-tier compensation with quadrature feed in the tier.

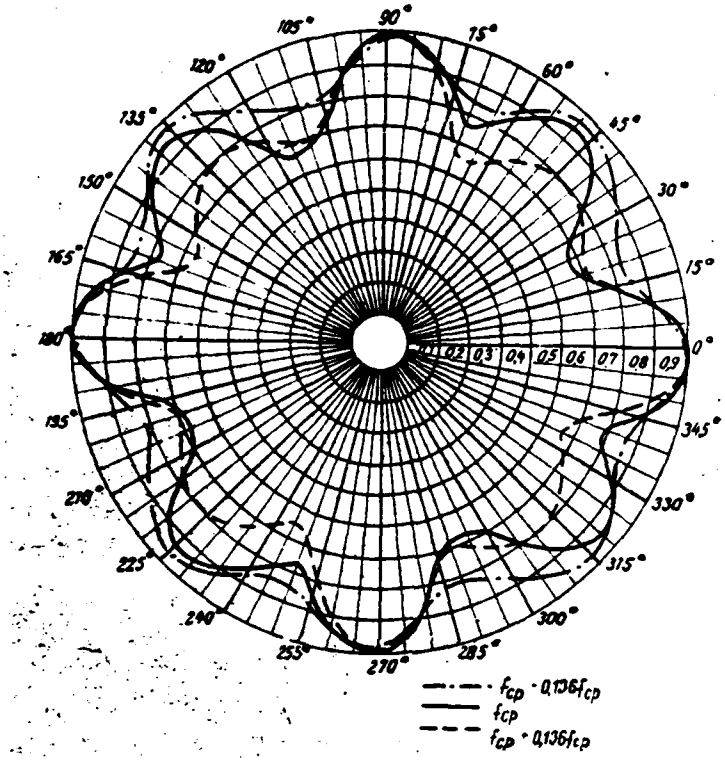

Fig. 15. Diagram of circular antenna with tangential shift of emitters in the horizontal plane.

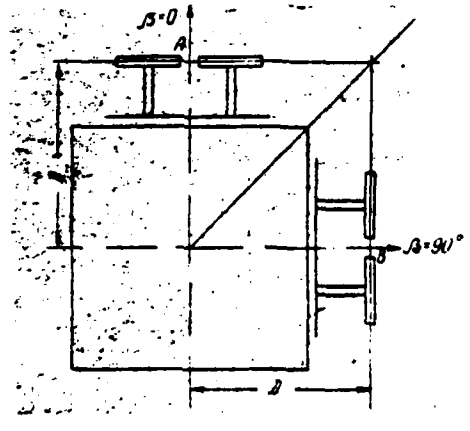

Fig. 16. Circular antenna with symmetrical placement of emitters.

It is quite evident that the selection of a certain angle of placement of the emitting elements relative to the axis of the support gives the necessary direction of the main lobe of the pattern. Thus, the introduction of phase shifts into the feed system of the tiers simultaneously solves two important problems: the accomplishment of inter-tier multiple compensation of the reflections, in accordance with the principles examined earlier, and inclination of the vertical pattern in order to best utilize the radiated energy.

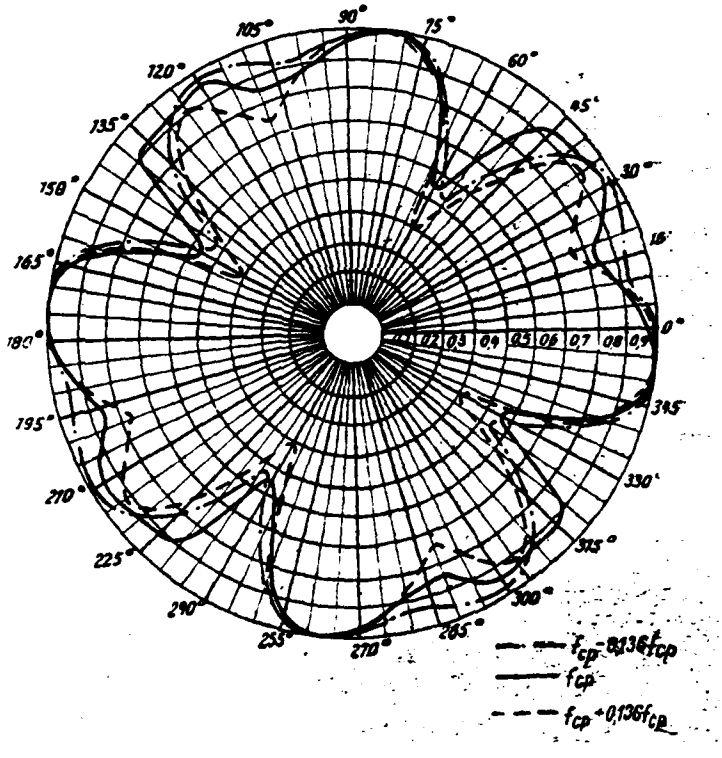

Fig. 17. Pattern of circular antenna in the horizontal plane with symmetrical placement of the emitting panels.

In all antennas, measures are also taken for the creation of a vertical characteristic of radiation which approaches a "cosecant" characteristic. This is achieved by both dephasing and feed of the tiers by unequal powers. Shown in Fig. 19 as an example is the vertical pattern of a typical antenna of range II.

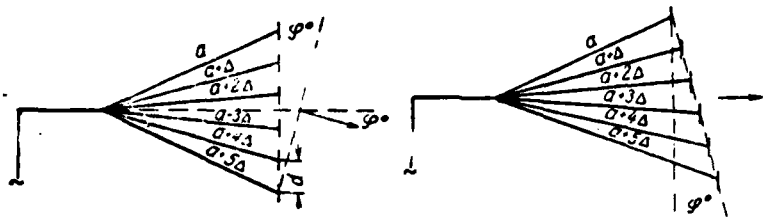

Fig. 18. Feed of tiers of antenna with increasing phase shift.

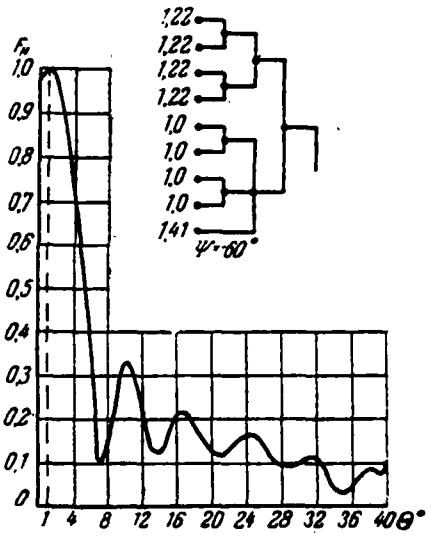

Fig. 19. Vertical diagram of typical range II antenna.

New Antenna Complex for Moscow Radio-Transmitting Television Station in Ostankino. The new antenna complex of the television station in Ostankino, mounted on a 533-meter free-standing reinforced concrete tower, will provide transmission of five television and six frequency-modulated broadcasting programs in the 1st (48.5-56.5 MHz), 3rd (76-84 MHz), 8th (190-198 MHz), 11th (214-222 MHz) and 33rd (566-574 MHz) television channels, and the frequency-modulated range (67-73 MHz).

In contrast to typical systems, as well as to the complex of the Leningrad Television Station, the antenna systems are made on a cylindrical free-standing steeple-like base 140 m high, rather than on prismatic supports. Insofar as the steeple is a solid tube of tiered profile, antennas were developed in which, in contrast to the so-called panel antennas, additional screens are absent. Such a solution made it possible to considerably reduce the weight and wind load on the support.

Television antennas of the 1st and 2nd channels and of frequency-modulated broadcasting were first made, in world practice, in the form of radial polyrod systems, located on cylinders of large cross-section. Such a design ensures a considerable decrease in weight and wind loads on the support, as well as simplification of operating conditions and maintenance, since the entire antenna feeder system is located inside the cylindrical support. Only the emitters are located on the outside, fastened using metallic and fiberglass insulators, which serve simultaneously as the casing for the emitter feed assembly.

The schematic of placement of all the antennas in the complex is shown in Fig. 20.

The antennas of the 8th and 11th channels are identical in their design and schematics. The emitters of these antennas are half-wave emitters with a built-on reflector. In order to improve the horizontal pattern, the dipoles are placed with a tangential shift.

The antenna of the 33rd channel is made in the form of a seven-tier structure of emitting panels, located around the central conduit four in a tier. Each panel contains eight tiers of wave dipoles. The exception is the middle tier, the panels of which contain only two tiers of dipoles. All of the panels are covered with casings of fiberglass to protect them from atmospheric precipitation and icing.

The feed schematics of all the antennas ensure multiple compensation of the reflections, inclination of the pattern in the direction of the horizon and elimination of zero radiation zones. The basic technical parameters of the antenna are given in Table 5. The main feeders, which connect the antennas to the transmitters and which have considerable dimensions (up to 450-500 m), ensure a high degree of matching and a high level of reliability.

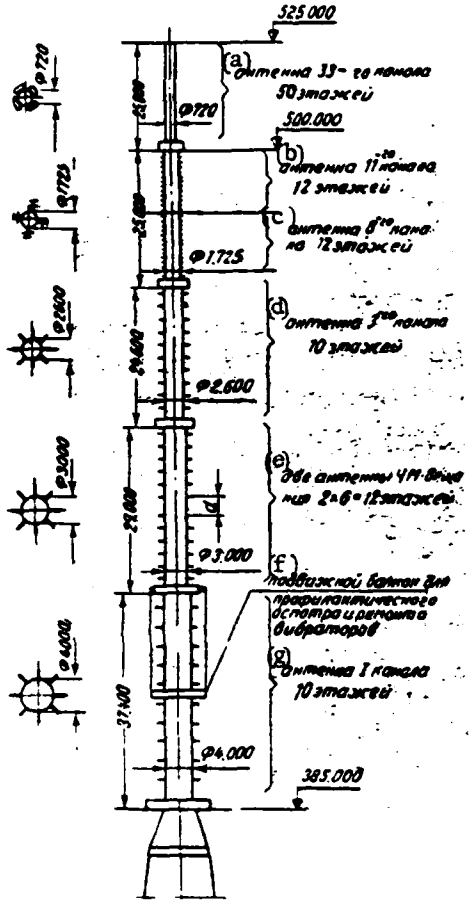

Fig. 20. Schematic of placement of antennas on 533-meter tower of the new Moscow Television Station in Ostankino.

Key: (a) antenna of 33rd channel, 50 tiers; (b) antenna of 11th channel, 12 tiers; (c) antenna of 8th channel, 12 tiers; (d) antenna of 3rd channel, 10 tiers; (e) 2 antennas of frequency-modulated broadcasting, 2 X 6=12 tiers; (f) movable platform for preventive inspection and repair of dipoles; (g) antenna of 1st channel, 10 tiers.

In order to increase reliability, the feeders are made air-tight with forced pumping of dry purified air, which precludes the possibility of an electrical breakdown as a result of contamination of the insulators or the entry of moisture.

Table 5.

(a) Общая высота опоры, м	525					
(b) Общая протяженность комплекса антенн, м	140					
(c) Количество антенн	7					
(d) Номер канала и тип антенны	(k) 1-й канал штыревая радиальн.	(l) 3-й канал штыревая радиальн.	(m) 8-й канал вибраторная безэкранная	(n) 11-й канал вибраторная безэкранная	(o) IV диапазон панельная	(p) УКВ ЧМ; штыревая радиальная (2 компл.)
(e) Число этажей	10	10	12	12	50	2×6 эт.
(f) Высота антенны, м	35	24	12,5	12,5	22	32
(g) Коэффициент усиления по сравнению с полуволновым вибратором	6	6	8	8	30	3
(h) Диаметр опоры, м	4	2,6	1,725		0,72	3,0
(i) Мощность передатчика (изображ./звук), квт	50/15		50/15		25/5	3×15
(j) Неравномерность диаграммы в горизонтальной плоскости, дб	±1,2		±2,5		±3	±1,2

KEY: (a) Total height of support, m; (b) Total extent of antenna complex, m; (c) Number of antennas; (d) Number of channel and type of antenna; (e) Number of tiers; (f) Height of antenna; (g) Coefficient of amplification as compared with half-wave dipole; (h) Diameter of support, m; (i) Power of transmitter (image/sound), kW; (j) Irregularity of pattern in horizontal plane, dB; (k) 1st channel, collapsible-whip radial; (l) 3rd channel, collapsible-whip radial; (m) 8th channel, dipole non-deflector; (n) 11th channel, dipole non-deflector; (o) Range IV, panel; (p) Ultra-short wave frequency-modulated, collapsible-whip radial (2 complexes).

Fig. 21. Antenna of 8th and 11th channels of the new Moscow Television Station on the adjusting stand.

Taking into account the difficulties in assembly and adjusting of the antennas under conditions of great height, the original control assembly and adjustment are carried out on special stands, located in direct proximity to the tower.

Shown in Fig. 21 are the antennas of the 8th and 11th channels on the adjusting stand, and in Fig. 22——the moment of assembly of the dipoles on the antenna of frequency-modulated broadcasting.

Evaluation of the effectiveness of operation of transmitting television antennas is usually carried out according to its amplification coefficient, which, in turn, is determined by the height of the antenna.

For multiprogram complexes of television antennas, the evaluation of their effectiveness may be carried out by means of comparing the summary dimensions of the antenna devices. In this respect, the complex of antenna structures of the Moscow Television Station in Ostankino will exceed all known foreign structures.

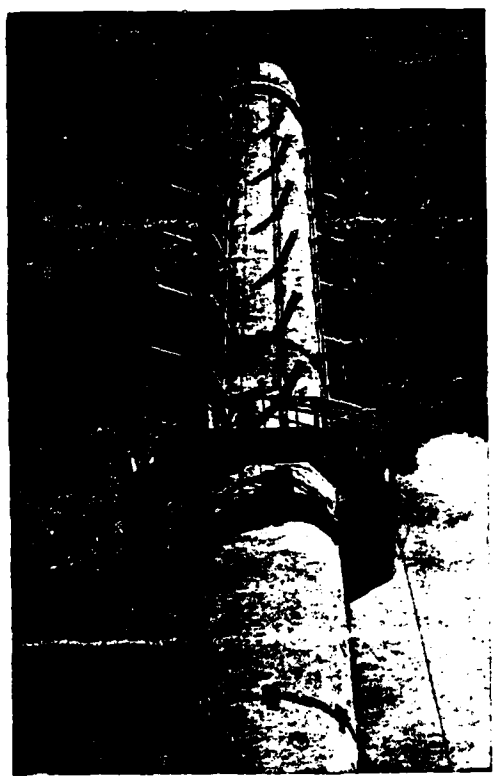

Fig. 22. Moment of assembly of antenna of frequency-modulated broadcasting of the new Moscow Television Station.

Thus, the complex of television antennas of the New York Television Station, which accomplishes broadcasting according to six television and three ultrashort wave frequency-modulated programs, has a dimension of 66 m, and the total height of the television tower of the television station, constructed in Montreal, is also designed, like that in Moscow, for five television and six

ultrashort wave frequency-modulated programs, which is a total of 110 m.

ЛИТЕРАТУРА

1. Рамлау П. Н. и Пистолькорс А. А. Советский патент № 17427, стр. 229, опубл. «Вестник Комитета по делам изобретений», 1930, № 9.
2. Пистолькорс А. А. и Нейман М. С. Прибор для непосредственного измерения кбв в фидерах. «Электросвязь», 1941, № 4.
3. Вольперт А. Р. Теоретическое и экспериментальное исследование фидерного рефлектометра. «Радиотехника», 1947, № 2.
4. Нейман М. С. Передающие телевизионные антенны. «Электросвязь», 1939, № 4.
5. Брауде Б. В. Новая широкополосная укв антенна для телевидения. «Радиотехника», 1947, № 7.
6. Masters R. W. The Super turnstile. Broodcast news, 42, 1946.
7. Трусканов Д. М. Способ питания турникетных антенн. Авторское свидетельство № 117712. Бюлл. № 2, 1959, стр. 38.
8. Трусканов Д. М. Новая схема питания телевизионных антенн с многократной компенсацией. Доклад на научной сессии НТО им. Попова, 1958 г. «Радиотехника», 1958, № 9, стр. 76—77.
9. Глаазман Э. С. Поглотитель фидерного эха для телевизионных передатчиков, «Радиотехника», 1959, № 2.
10. Крылов А. Н. Лекции о приближенных вычислениях. Изд. 5-е. М.-Л., Госуд. изд. техн.-теорет. литерат., 1950.

DISCRIMINATION OF HOLOGRAM AND ANTENNA THEORY

A. A. Pistol'kors

This article is devoted to the theoretical study of the matter of the discrimination of the hologram during image reproduction. A two-dimensional electrodynamic problem is examined. Conditions are established for the correct reproduction of an image of a luminous line with the use of planar and cylindrical reference flows. Studied on their basis is the discrimination of the hologram in the direction parallel to its plane. A similarity is noted between the obtained expression and the integral equation of a linear antenna, which makes it possible to utilize the well developed theory of directional effect of antennas for the purposes of the present study. Using this theory, one may specifically show that the maximum resolution in the plane parallel to the hologram is equal to the wave length.

The discrimination in the direction perpendicular to the plane of the hologram proves to be much worse.

Derivation of the Basic Expression for the Electrical Field of the Image

One of the uses of holography is the production of a three-dimensional image of some object or another. For this purpose, an object P (Fig. 1) is illuminated by a monochromatic light source. The light reflected from the object strikes a photographic plate AB, which is simultaneously illuminated by a reference flow

of light S_1 from the very same source (Fig. 1a). The resulting photograph (hologram) is then transilluminated by a reference flow S_2 (Fig. 1b) of monochromatic light of the very same wave length. In this case, two types of beams emanate from the

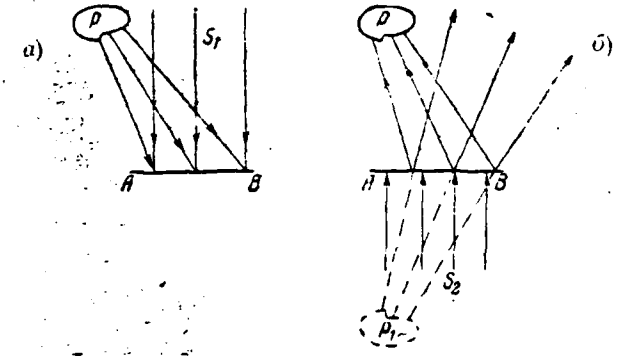

Fig. 1. (a) light flows which reach the hologram during photographing; (b) light flows with the formation of an image using the hologram.

hologram. Some beams (convergent) form a so-called actual image of the object P, while others (divergent) correspond to a virtual image of the object P_1, which appears to the observer to be located behind the hologram.

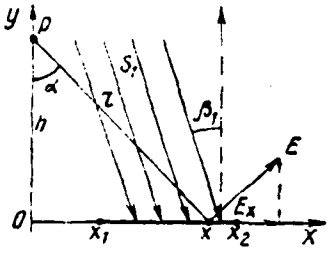

Fig. 2. Calculation of the electrical field on the surface of the hologram.

In the current study (the content of which is set forth briefly in study [1]), we will apply the methods of electrodynamics to the study of the discrimination of the hologram; first, it will be necessary to ascertain the requirements which should be placed on the reference flows in order to obtain an undistorted image.

In order to simplify the matter, we will examine a two-dimensional problem, in which the luminous point is replaced with a luminous line, parallel to the z-axis. In this case, the hologram should be represented in the form of an infinite band with a width 1. If, along the z-axis, the parameters of the system are constant,

then one may limit oneself to the examination of the processes which occur in the plane XOY. In it, the point P (Fig. 2) corresponds to the luminous line, and the line x_1x_2 corresponds to the cross-section of the hologram. The intensity of the electrical field E_x, created by the luminous line, on the surface of the photographic plate at the point x is determined by the cylindrical wave function and the angle of incidence of the wave α:

$$E_x = \frac{A e^{-ikr}}{\sqrt{kr}} \cos\alpha = \frac{A e^{-ikr}}{\sqrt{kr}} \frac{h}{r}, \qquad (1)$$

where $r=\sqrt{h^2+x^2}$,

h is the ordinate of the luminous point (its abscissa is equal to 0),

$k = 2\pi/\lambda$ is the wave number,

A is the coefficient of proportionality, which has the dimensionality of the intensity of the electrical field E.

The time multiplier $e^{i\omega t}$ is omitted in expression (1).

Let the field, created by the flow S_1 on the surface of the photographic plate, be

$$E_{S_1} = E_1 f_1(x) e^{-i\varphi_1(x)}. \qquad (2)$$

Here, the coefficient E_1 has the dimensionality of E; $f_1(x)$ is a dimensionless positive function. In the specific case of a planar wave, incident at an angle β_1 (Fig. 2),

$$\varphi_1(x) = kx \sin\beta_1.$$

Combining the fields E_{S_1} and E_x, and assuming that the density of the photographic film is proportional to the square of the summary intensity of the electrical field, we obtain the following

for the coefficient of absorption of light Q(x) on the surface of the film

$$Q(x) \sim E_1^2 f_1^2(x) + \frac{2E_1 f_1(x) Ah}{\sqrt{\kappa r^3}} \cos[\kappa r - \varphi_1(x)] + \frac{A^2 h^2}{\kappa r^3}. \qquad (3)$$

The produced negative is usually transilluminated in order to reproduce the image. This is permissible when $f_1(x)$=const, since then, the use of the negative instead of the positive is equivalent to the change in phase of the field by π, which does not show up on the reproduced image. With $f_1(x) \neq$const, it is necessary to transilluminate the positive. Let the field, created in this case by the reference flow S_2 on the surface of the positive, be

$$E_{S_2} = E_2 f_2(x)\, e^{-i\varphi_2(x)}.$$

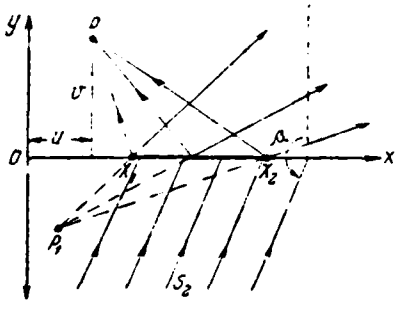

Fig. 3. Determination of the position of the luminous point, formed during transillumination of the hologram.

Just like for the flow S_1, with irradiation of the hologram by a planar wave, incident at an angle β_2 to the external normal (Fig. 3),

$$\varphi_2(x) = \kappa x \sin\beta_2.$$

The field created by the middle term of expression (3)[1] at the point x=u, y=v (Fig. 3), is

$$E_u = E_n \kappa h^2 \int_{x_1}^{x_2} \frac{f_1(x) f_2(x)}{\sqrt{\kappa r^3}} \frac{e^{-i\kappa r_1}}{\sqrt{\kappa r_1^3}} \cos[\kappa r - \varphi_1(x)]\, e^{-i\varphi_2(x)}\, dx =$$

$$= E_n \frac{h^2}{2} \left[\int_{x_1}^{x_2} \frac{f_1(x) f_2(x)}{\sqrt{r^3 r_1^3}} e^{i\kappa(r-r_1) - i\varphi_1(x) - i\varphi_2(x)}\, dx + \right.$$

$$\left. + \int_{x_1}^{x_2} \frac{f_1(x) f_2(x)}{\sqrt{r^3 r_1^3}} e^{-i\kappa(r+r_1) + i\varphi_1(x) - i\varphi_2(x)}\, dx \right] = E_{u1} + E_{u2}. \qquad (5)$$

[1] Here, we will not dwell on the methods of spatial separation of the image and the constant component of the light flow, characterized by the first and third terms in expression (3).

Here, E_n is the coefficient of proportionality with the dimensionality of E;

$$r_i = \sqrt{v^2 + (x-u)^2}.$$

The first term ($E_{И1}$) is the field of the actual image (convergent beams). The second term corresponds to the divergent beams, by continuing which beyond the limits of the hologram (Fig. 3), we produce the virtual image. The virtual field $E_{И2}$, which corresponds to this image, we will obtain by substituting the values of e^{+ikr_i} in place of e^{-ikr_i} into the expression for $E_{И2}$. Then

$$E'_{И2} = E_n \frac{h^2}{2} \int_{x_1}^{x_2} \frac{f_1(x) f_2(x)}{\sqrt{r^3 r_i^3}} e^{-i\kappa(r-r_i)+i\varphi_1(x)-i\varphi_2(x)}\, dx. \qquad (6)$$

Requirements for Reference Flows

In order to determine where the luminous line of the actual image will form, we will find that point u, v in which the waves, incoming from the elements of a potentially larger segment of the x-axis, coincident with the hologram, are combined into a similar or close phases. This means that the exponent in the expression for $E_{И1}$:

$$\psi(x) = \kappa(r - r_i) - \varphi_1(x) - \varphi_2(x) \qquad (7)$$

should be a constant magnitude, or weakly changing function, for all values of x within the limits $x_2 \geq x \geq x_1$. We will expand the function $\Psi(x)$ into a Taylor series:

$$\psi(x) = \psi(x_0) + \frac{x - x_0}{1!}\psi'(x_0) + \frac{(x-x_0)^2}{2!}\psi''(x_0) + \ldots.$$

Here, x_0 is the abscissa of the middle of the hologram.

If the luminous point is correctly reproduced, then the phase of $\Psi(x)$ should be constant for all values of x, and, consequently, all derivatives of this function will be equal to zero. With incorrect reproduction of the point, one may find

its coordinates u and v, proceeding from the equality to zero of at least the first two derivatives of $\Psi(x)$ with $x=x_0$, i.e., solving the following equations relative to u and v

$$\psi'(x_0) = \psi''(x_0) = 0. \tag{8}$$

In this case, the maximum permissible width of the hol[illegible]m x_2-x_1 is determined from the requirement that, at the point of reproduction of the waves from its extreme points (x_1 and x_2), they differed from the phase, created by x_0, by no more than some acceptable given magnitude.

By designating $\phi_1(x)+\phi_2(x)$ via $\phi(x)$, we obtain

$$\psi'(x_0) = \frac{x_0}{\sqrt{h^2+x_0^2}} - \frac{x_0-u}{\sqrt{v^2+(x_0-u)^2}} - \varphi'(x_0) = 0. \tag{9}$$

If the direction to the luminous point P from the middle of the hologram during photographing was determined by the angle α_0, with respect to the normal, and the direction to the formed point P_1 during transillumination [illegible] determined by the angle γ_0 (Fig. 4), then, from equation (9), it follows that

$$\sin\gamma_0 = \sin\alpha_0 - \varphi'(x_0) = 0. \tag{10}$$

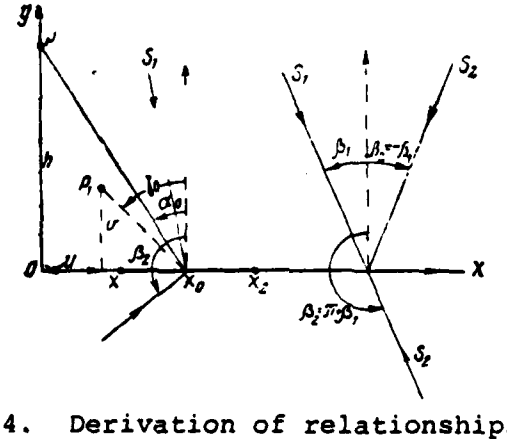

Fig. 4. Derivation of relationships, the fulfillment of which is necessary for the production of an undistorted image.

Consequently, the actual image is formed in the correct

direction only in that case when

$$\varphi'(x_0) = 0$$

and, specifically, when $\phi(x) = \phi_0 = \text{const}$.

For $\Psi''(x_0)$, we obtain

$$\psi''(x_0) = h^2\left(h^2 + x_0^2\right)^{-\frac{3}{2}} - v^2\left[v^2 + (x_0 - u)^2\right]^{-\frac{3}{2}} - \varphi''(x_0) = 0 \tag{11}$$

or, switching to angles,

$$\frac{\cos^3 \alpha_0}{h} - \frac{\cos^3 \gamma_0}{v} - \varphi''(x_0) = 0. \tag{12}$$

Having determined the angle γ_0 from equation (10), we find the coordinate v of the formed point from equation (12).

We will examine the case of reference flows in the form of planar waves, incident at angles β_1 and β_2. Then

$$\varphi(x) = \kappa p x + \varphi_0, \tag{13}$$

where $$p = \sin\beta_1 + \sin\beta_2.$$

In this case,

$$\varphi'(x) = p, \quad \varphi''(x) = 0$$

and the solutions of the equations (8) are written as:

$$\left.\begin{aligned} &\sin\gamma_0 = \sin\alpha_0 - p \\ &v = h\frac{\cos^3\gamma_0}{\cos^3\alpha_0}, \quad x_0 - u = v\,\mathrm{tg}\,\gamma_0 \end{aligned}\right\}, \tag{14}$$

and the distance from the image to the point x_0 will be

$$x_0 P_1 = h\frac{\cos^3\gamma_0}{\cos^3\alpha_0}.$$

In order that the image be formed in the correct direction, in accordance with what has been said above, it should be that

$$\psi'(x) = p = \sin\beta_1 + \sin\beta_2 = 0.$$

This equality may be fulfilled in two cases:

$$\beta_2 = -\beta_1$$

and

$$\beta_2 = \pi + \beta_1.$$

In the former case, the reproducing reference flow S_2 falls on the front of the hologram (Fig. 4), while the actual image is formed on its rear side. It is not difficult to see that, in this case, it will be a mirror image with respect to the initial object. The direct image of the object will be obtained by illuminating the hologram from the rear, when $\beta_2=\pi+\beta_1$. In this case,

$$\gamma_0 = \alpha_0,\ v = h,\ u = 0$$

and the coordinates of the formed point will coincide with the coordinates of the initial point. All of the derivatives of $\Psi(x)$ will automatically be equal to zero, and the waves arriving from any elements of the x-axis will combine in phase at the point which corresponds to the initial point.

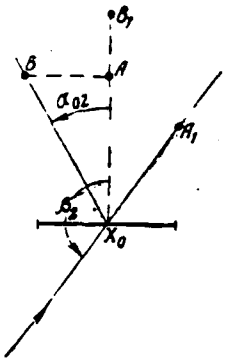

Fig. 5. Example of distortions of the reproduced image, obtained with incorrect selection of the angle of incidence of the planar reference flow, which trans-illuminates the hologram.

If $p\neq 0$, then the image will be turned and distorted. As an example, we will take $\beta_1=0$, $\sin\beta_2\neq 0$. Then,

$$\sin\gamma_0 = \sin\alpha_0 - \sin\beta_2.$$

Point A (Fig. 5), for which $\alpha_{01}=0$, will be deflected at an angle $\gamma_0=-(\pi-\beta_2)$, and will be located a distance $x_0A_1=h\cos^2\beta_2$ from the middle of the hologram. Point B, at which $y=h$ and $\alpha_{02}=\pi-\beta_2$ (Fig. 5), will have $\gamma_{02}=0$, and the distance of its image B_1 to the point x_0 will be

$$x_0B = \frac{h}{-\cos^3\beta_2}.$$

If, in the initial image, $x_0A/x_0B=-\cos\beta_2$, then, in the formed image, $x_0A_1/x_0B_1=-\cos^5\beta_2$, i.e., the mutual placement of points A and B will be incorrectly reproduced.

Similar conclusions may be obtained for the virtual image as well, but here

$$p = \sin\beta_2 - \sin\beta_1,$$

and in order to have no distortions (so that p=0), it is necessary

to fulfill one of the two equalities:

$$\beta_2 = \beta_1$$

or

$$\beta_2 = \pi - \beta_1.$$

In the former case, the hologram is illuminated from the front, and the image is examined from its rear side. The image will be direct (not mirror).

In the latter case — the mirror virtual image — the planar reference flow illuminates the rear side of the hologram, and the observer is located to the front.

From what has been said, it follows that, with oblique illumination of the photographic plate by a planar reference flow ($\beta_1 \neq 0$), one may select the angle of incidence β_2 of the planar flow during reproduction so that the actual image would be undistorted, and the virtual image would be distorted, or vice versa. Both images will be simultaneously undistorted only with normal incidence of the reference planar flows, when $\beta_1 = 0$, and $\beta_2 = \pi$ or 0.

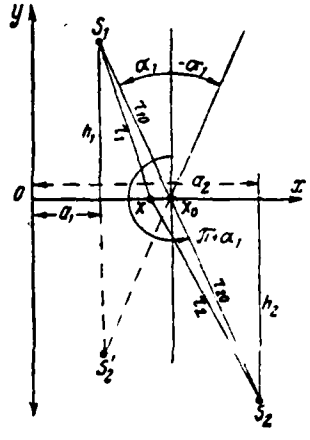

Fig. 6. Case of point sources of reference light flows.

The requirement p=0, the fulfillment of which is necessary for the production of an undistorted image, should be taken into account during the examination of the matter of the discrimination of the hologram.

We will now examine the case when radiation from a point source is utilized as the reference light flow. In this case (Fig. 6),

$$E_{S_1} = \frac{A_1}{\sqrt{r_1}} \frac{h_1}{r_1} e^{-ikr_1},$$

where

$$r_1 = \sqrt{h_1^2 + (a_1 - x)^2}.$$

By comparing the obtained expression with expression (2), we note that, in the given case:

$$f_1(x) = \frac{A_1}{\sqrt{\kappa r_1}} \frac{h_1}{r_1},$$
$$\varphi_1(x) = \kappa r_1.$$

Accordingly, for the reference flow during reproduction (Fig. 6):

$$f_2(x) = \frac{A_2}{\sqrt{\kappa r_2}} \frac{h_2}{r_2},$$
$$\varphi_2(x) = \kappa r_2.$$

It was shown earlier that a necessary condition for the correct reproduction of the actual image should be

$$\varphi(x) = \varphi_1(x) + \varphi_2(x) = \text{const.}$$

In the given case, when $\phi_1(x)+\phi_2(x)=k(r_1+r_2)$, this is impossible, and one may only speak of the relatively correct reproduction of the image with restricted dimensions of the hologram. It is necessary, for this purpose, that equations (10) and (11) be fulfilled for the middle of the hologram (point x_0), or, otherwise, that

$$\varphi'(x_0) = 0$$

and

$$\varphi''(x_0) = 0.$$

The former of these equations gives

$$\frac{a_1 - x_0}{\sqrt{h_1^2 + (a_1 - x_0)^2}} + \frac{a_2 - x_0}{\sqrt{h_2^2 + (a_2 - x_0)^2}} = 0$$

or

$$\sin\alpha_2 = -\sin\alpha_1.$$

One may satisfy this requirement by placing the point sources of the reference flows so that the directions to them from the point x_0 would make angles from the normal to the hologram α_1 and $\alpha_2=-\alpha_1$ or α_1 and $\alpha_2=\pi+\alpha_1$ (Fig. 6).

The latter equation leads to the following

$$\frac{h_1^2}{\left[h_1^2+(a_1-x_0)^2\right]^{\frac{3}{2}}}+\frac{h_2^2}{\left[h_2^2+(a_2-x_0)^2\right]^{\frac{3}{2}}}=\frac{\cos^2\alpha_1}{h_1}+\frac{\cos^2\alpha_2}{h_2}=0.$$

With the selection of angles α_1 and α_2, given above, it is impossible to satisfy this requirement using real values of h_2 and, consequently, the requirement $\phi''(x_0)=0$ may not be realized. But, in that case, which follows from equation (12), the ordinate of the reproduced point will not be equal to h, as well as its abscissa to zero, and the image of the reproduced object will be distorted. The distortions will evidently be less the closer $\phi''(x_0)$ is to zero, and, specifically, the greater h_1 and h_2 are as compared to h, i.e., the farther the sources of the reference radiation are from the hologram. From here, it follows that accurate reproduction of the actual image may be obtained only using reference flows in the form of planar waves.

At the same time, the virtual image may be obtained without distortion also using point sources of reference light flows. In this case, it is sufficient that the reproducing source be located at the point of the former, which forms the phase front (direct virtual image), or is symmetrical relative to it (Fig. 6, dotted line); then, we obtain a mirror virtual image. In both cases, $r_1=r_2$, and since $\phi(x)=\phi_1(x)-\phi_2(x)$ for the virtual image, then $\phi(x)=k(r_1-r_2)=0$.

Discrimination of the Hologram Along the x-Axis

We will investigate the field intensity at small distances ξ from the reproduced point along the line which passes through this point parallel to the x-axis. For this purpose, one may utilize the first term in expression (5), in which we will now assume that $\phi_1(x)+\phi_2(x)=0$, $f_1(x)f_2(x)=f(x)$ and $r_i=\sqrt{y^2+(x-\xi)^2}$. Then

$$r-r_i\approx\sqrt{h^2+x^2}-\sqrt{h^2+x^2}\left(1-\frac{x\xi}{h^2+x^2}\right)=\frac{x\xi}{\sqrt{h^2+x^2}}, \tag{16}$$

if $\xi \ll r$, which corresponds to the posed problem. In this case, $\sqrt{r^3r_i^3}\approx r^3$. Since $r=h/\cos\alpha$, and $x/\sqrt{h^2+x^2}=\sin\alpha$, then

$$E_\xi = \frac{E_n h^2}{2}\int_{x_1}^{x_2} f(x)\,\frac{e^{\frac{i\kappa x\xi}{\sqrt{h^2+x^2}}}}{r^3}\,dx = \frac{E_n}{2h}\int_{x_1}^{x_2} f(x)\cos^2\alpha\, e^{i\kappa\xi\sin\alpha}\,d\alpha.$$

But, x=h tg α and dx=hdα/cos^{2}α; therefore, if f(x)=F(α), then

$$E_\xi = 0{,}5\,E_n\int_{\alpha_1}^{\alpha_2} F(\alpha)\,e^{i\kappa\xi\sin\alpha}\cos\alpha\,d\alpha \tag{17}$$

or, assuming sin α=u and F(α)=θ(u),

$$E_\xi = 0{,}5E_n\int_{u_1}^{u_2}\theta(u)\,e^{i\kappa\xi u}\,du. \tag{18}$$

The very same result is obtained for the virtual image, if $\phi_1(x)-\phi_2(x)=0$.

Expression (18) is similar to the formula for the beam pattern along the field D(Θ) of a linear antenna, located along the z-axis (Fig. 7):

$$D(\Theta) = \kappa M\int_{z_1}^{z_2} F(z)\,e^{i\kappa z\sin\Theta}\,dz. \tag{19}$$

Here, $F(z)=f(z)e^{i\phi(z)}$ is the function of distribution of the current (field) along the antenna,

z_1 and z_2 are the coordinates of its beginning and end,

Θ is the angle between the direction to the point of observation and the normal to the axis of the antenna,

M is the scale coefficient, which has a dimensionality E.

The coordinate u, the function θ(u) and the magnitude ξ in expression (18) correspond to the coordinate z, the function F(z) and the magnitude sin Θ in expression (19), with only that difference that u and sin Θ are dimensionless, while z and ξ have dimensionality of length. What has been said makes it possible to utilize the well developed theory of directed effect of antennas for the analysis of expression (18).

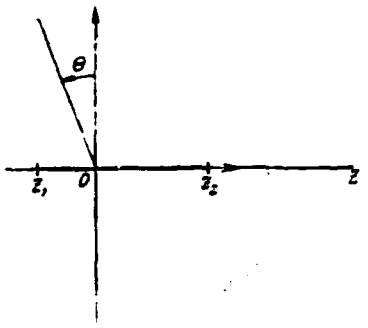

Fig. 7. The expression for the beam pattern of a linear antenna.

Since $\theta(u)$ is a positive real function of u, then (18) corresponds to the beam pattern of a cophasal antenna. In this case, insofar as the magnitude of ξ is not restricted, and $|\sin\alpha| \leq 1$, the indicated expression is equivalent to the beam pattern which encompasses not only real, but also virtual angles $\theta(|\sin\theta|>1)$. The beam patterns in the region of virtual angles are also examined in the theory of antennas, since they play an important role in the determination of the wattless power of the antenna.

We will examine the case of uniform illumination of the hologram by the reference flows S_1 and S_2; then, $\theta(u)=\text{const}=1$, and

$$E_\xi = 0{,}5E_n \int_{u_1}^{u_2} e^{i\kappa\xi u}\,du = 0{,}5\,E_n e^{i\kappa\xi\frac{u_1+u_2}{2}} \frac{\sin\kappa\xi\frac{u_2-u_1}{2}}{\frac{\kappa\xi}{2}}. \qquad (20)$$

It is evident from Fig. 8 (curve 1) that the amplitude of the field intensity in the region of the reproduced point changes according to the law $\left|\frac{\sin px}{x}\right|$, which is characteristic for the beam pattern of a cophasal antenna with a current amplitude which is unchanged with length. The point is reproduced in the form of a large surge of intensity of the electrical field, accompanied by smaller surges, which are adjacent to it. The maximum value of the field intensity E_0 is determined from expression (20) with $\xi\to 0$:

$$E_0 = 0{,}5\,E_n(u_2-u_1) = 0{,}5E_n(\sin\alpha_2-\sin\alpha_1). \qquad (21)$$

In antenna theory, resolution of the beam pattern is understoc to mean the angle within the limits of which the main lobe drops to

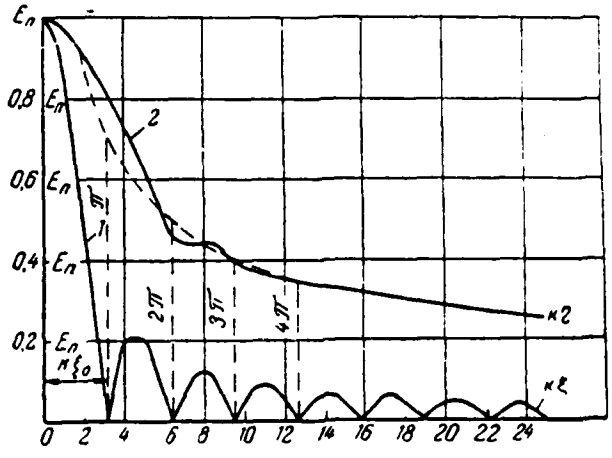

Fig. 8. Curves of intensity of electrical field, created by the hologram in the region of the reproduced luminous point; curve 1 corresponds to the distribution of the field along the ξ-axis, parallel to the x-axis, and curve 2 gives the distribution of the field along the y-axis (η is the distance from the ordinate of the reproduced point).

half power. The discrimination determined thusly characterizes the possibility of picking out near sources of radiation. In the case examined here, it is more advisable, evidently, to understand discrimination to mean the width $2\xi_0$ of the main surge of intensity of the field at the zero point (Fig. 8), which characterizes the "extent" of the reproduced point. Assuming that

$$\sin \kappa \xi_0 \frac{u_2 - u_1}{2} = \sin \pi = 0 \text{ и } x_2 > x_1,$$

we find

$$2\xi_0 = \frac{2\lambda}{u_2 - u_1} = \frac{2\lambda}{\sin \alpha_2 - \sin \alpha_1} = \frac{2\lambda}{\frac{x_2}{\sqrt{h^2 + x_2^2}} - \frac{x_1}{\sqrt{h^2 + x_1^2}}}. \quad (22)$$

With symmetrical placement of the hologram relative to the luminous line, when $x_1 = -x_2$,

$$E_0 = E_n \sin \alpha_2 \quad (23)$$

and

$$2\xi_0 = \frac{\lambda}{\sin \alpha_2} \text{ [1)]} = \lambda \frac{\sqrt{h^2 + x_2^2}}{x_2}. \tag{24}$$

We will evidently obtain maximum resolution with $x_2 \to \infty$ or $\sin \alpha_2 \to 1$. In this case (to which curve 1 in Fig. 8 corresponds)

$$2\xi_0 = \lambda. \tag{25}$$

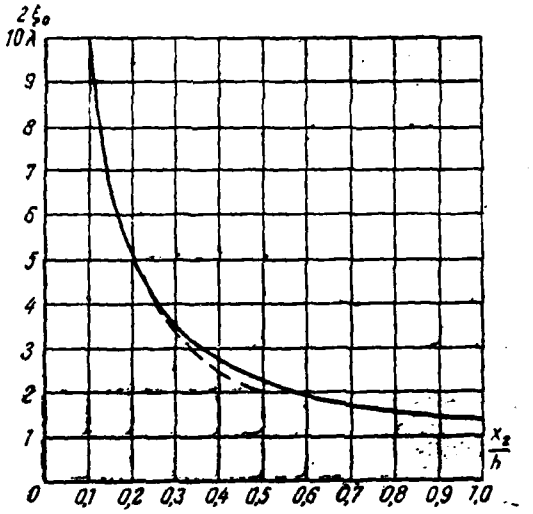

Fig. 9. Dependence of the resolution of the hologram on its dimensions with symmetrical placement of the hologram relative to the luminous point; $2\xi_0$ is the width of the main maximum in wave lengths.

Shown in Fig. 9 is the dependence of the resolution on the dimensions of the hologram with its symmetrical placement relative to the luminous line. With small dimensions of the hologram

$$2\xi_0 \approx \lambda \frac{h}{x_2}; \tag{26}$$

the dotted line in Fig. 9 corresponds to this expression.

It follows from what has been said that closer illuminated objects will be resolved better than further objects, since, for the former, the relationship h/x_2 is less than for the latter.

---

[1] A similar expression without derivation is given in study [2].

With nonsymmetrical placement of the reproduced line relative to the hologram, the resolution is impaired with an increase in the angle α_0. Given in Fig. 10 are the curves of the dependence of the resolution on this angle for holograms of various dimensions.

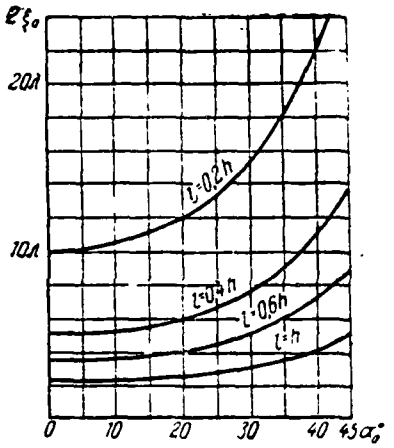

Fig. 10. Dependence of the resolution on the angle α_0, formed by the direction to the luminous point from the center of the hologram with the normal to its surface, for holograms of various widths l; $2\xi_0$ is the width of the main maximum.

We would note that, for the switch to discrimination according to half power $2\xi_p$, it is sufficient to multiply the obtained results by a multiplier equal to 4/9. Thus,

$$2\xi_p = \frac{8}{9}\xi_0. \qquad (27)$$

All that has been said concerns the uniform illumination of the hologram by reference flows. A shortcoming of similar illumination is the comparatively high level of secondary surges of field intensity.

With other laws of illumination, the level of secondary surges may be reduced because of slight impairment of the discrimination. Some of the relevant data here, which are known from antenna theory, are given in the Table.

One should also avoid those laws of illumination with which secondary radiation increases in the range of values of ξ which correspond to virtual angles. Although such laws are often applicable in radio technology, they are inapplicable in holography.

It is necessary to bear in mind that the conclusions obtained here are correct for holograms with ideally flat surfaces. Actually, these surfaces, from the point of view of light wave length, are quite rough. The effect of irregularities on the

surface of the hologram on the quality of the image may be taken into consideration using methods developed in studies on statistical evaluation of antenna parameters.

Table

(a) Распределение поля		(b) Относительная ширина главного всплеска	(c) Уровень первого побочного всплеска в % к главному
	(d) Равномерное	1	21,2
	(e) Косинусоидальное	1,36	7,0
	(f) Треугольное	1,46	4,5

Key: (a) distribution of field; (b) relative width of main surge; (c) level of first secondary surge in % of main; (d) uniform; (e) cosinusoidal; (f) triangular.

Discrimination of the Hologram Along the y-Axis

Again utilizing expression (5), we will calculate the field intensity at the point with coordinates x=0, y=h-η, where η is a small magnitude. Reasoning the same as in the previous section, we obtain

$$E_\eta = 0{,}5\,E_\Pi h^2 \int_{x_1}^{x_2} r^{-3}\, e^{\frac{i\kappa h\eta}{\sqrt{h^2+x^2}}} f(x)\,dx = 0{,}5E_\Pi \int_{\alpha_1}^{\alpha_2} F(\alpha)\, e^{i\kappa\eta\cos\alpha}\cos\alpha\, d\alpha\,. \qquad (28)$$

One may calculate E_η utilizing expansion according to Besselian functions:

$$e^{i\kappa\eta\cos\alpha} = J_0(\kappa\eta) - 2J_2(\kappa\eta)\cos 2\alpha + 2J_4(\kappa\eta)\cos 4\alpha - \ldots + i\,2[J_1(\kappa\eta)\cos\alpha - J_3(\kappa\eta)\cos 3\alpha + J_5(\kappa\eta)\cos 5\alpha - \ldots \qquad (29)$$

It follows from this expansion that there will be no pure zeros of the field intensity along the y-axis. The maximum field

intensity (at the point O, h) will be

$$E_0 = 0{,}5E_n \int_{\alpha_1}^{\alpha_2} F(\alpha)\cos\alpha\, d\alpha.$$

With

$$F(\alpha) = \text{const} = 1 \quad E_0 = 0{,}5E_n(\sin\alpha_2 - \sin\alpha_1)$$

in accordance with expression (21).

At a sufficient distance from the maximum, when $k\eta$ is a comparatively large magnitude, integral (28) may be calculated by the method of the stationary phase, if the point of the stationary phase $\alpha=0$ falls within the limits of integration. In this case

$$|E_\eta| \approx 0{,}5E_n \sqrt{\frac{\lambda}{r_1}}\, F(0). \qquad (30)$$

Expression (30) is correct for those values of shifting η with which a sufficiently large number of periods of the oscillating function $e^{ik\eta\cos\alpha}$ are contained within the limits of integration.

With symmetrical placement of the luminous point relative to the hologram ($\alpha_1=-\alpha_2$) and with $F(\alpha)=1$

$$E_0 = E_n \sin\alpha_2.$$

We obtain the greatest discrimination with infinite width of the hologram, when $\alpha_2=\pi/2$. The curve of field intensity for this case is designated by the number 2 in Fig. 8. It is constructed according to the formula

$$E_\eta = E_n\left[J_0(\kappa\eta) - \frac{2}{1\cdot3}J_2(\kappa\eta) - \frac{2}{3\cdot5}J_4(\kappa\eta) - \frac{2}{5\cdot7}J_6(\kappa\eta) - \ldots\right] + i\frac{\pi E_n}{2}J_1(\kappa\eta),$$

obtained from expression (29). As we see, curve 2 differs severely from curve 1 of the field intensity along the ξ-axis. A slowly dropping tail is characteristic, because of which, even at a distance 1.5 λ from the maximum (with $k\eta=3\pi$), the field intensity decreases to only 40%.

Shown by the dotted line in Fig. 8 is the curve of field intensity calculated according to the method of the stationary phase; as we see, it provides good coincidence with the precise curve with $k\eta > 4\pi$. With symmetrical placement of the hologram and with integration within the limits from 0 to α_2, the argument of the oscillating function changes from $k\eta$ to $k\eta\cos\alpha_2$; consequently, over the length $k\eta(1-\cos\alpha_2) = 2k\eta\sin^2\frac{\alpha_2}{2}$, there should be n/2 periods, from which

$$k\eta_{\text{мин}} = \frac{n\pi}{2\sin^2\frac{\alpha_2}{2}}$$

or, for small α_2 $k\eta_{\text{мин}} = 2n\pi\left(\frac{h}{x_2}\right)^2$.

For the curves in Fig. 8, $\sin^2\frac{\alpha_2}{2} = 0.5$ and $k\eta_{\text{мин}} = 4\pi$, from which the minimum required number of periods n=4. Consequently, for symmetrical placement of a hologram of any width

$$k\eta_{\text{мин}} = \frac{2\pi}{\sin^2\frac{\alpha_2}{2}}.$$

In this case, $E_\eta = 0.5E_\Pi\sin\frac{\alpha_2}{2}$ and $\frac{E_\eta}{E_0} = \frac{0.25}{\cos\frac{\alpha_2}{2}}$.

In view of the fact that, with small width of the hologram, $\cos\frac{\alpha_2}{2} \approx 1$, $k\eta_{\text{мин}}$ corresponds to the distance at which the field intensity drops to one fourth of the maximum value. Since $k\eta_{\text{мин}} \approx 8\pi\left(\frac{h}{x_2}\right)^2$, this distance increases rapidly with a decrease in the width of the hologram, and the curve E_η becomes all the more blurred.

We would note that, because of the parity relative to α,

$$\int_0^{\alpha_2} e^{ik\eta\cos\alpha}\cos\alpha\,d\alpha = 0{,}5\int_{-\alpha_2}^{\alpha_2} e^{ik\eta\cos\alpha}\cos\alpha\,d\alpha.$$

This means that the curve of field intensity, created by a nonsymmetrically located hologram (when α changes from 0 to α_2), is the same as in a symmetrically placed hologram of twice the

width; only the amplitude of the field decreases by twice.

As we see, the discrimination of the hologram along the y-axis is considerably worse than along the x-axis, especially with small dimensions of the holograms. Therefore, it is more advantageous to view the image from those positions with which the line of sight is directed roughly along the y-axis, and the image develops basically in the plane parallel to ZOX. Practically, it is more convenient to realize such coverage with respect to the virtual, rather than the actual, image.

ЛИТЕРАТУРА

1. Пистолькорс А. А. О разрешающей способности голограммы. Доклады Академии наук, т. 172. 1967 № 2, стр. 334—337.
2. Leith E. N., Upatniks J., Hildebrand B. P., Haines K. Requirements for a wavefront reconstruction television facsimile system. «J. Soc. Mot. Pict. Telev Eng.», 1965, v. 74, № 10, pp. 893—896. Перевод в «Зарубежной радиоэлектронике» вып. 5, май 1966, стр. 3—11.

RADIATION OF AN ANTENNA IN THE FORM OF A RIBBED SHAFT OF FINITE LENGTH

G. D. Malushkov

The method of integral equations of the first order is used to solve the problem of excitation of an impedance cylinder of finite length by a short ($l<\lambda/4$) symmetrical electrical dipole with sinusoidal distribution of the outside current. The dipole is located on the axis of rotation of the cylinder, and is perpendicular to it. Also given are the procedure and some results of calculation of the current distributions on the surface of the impedance cylinder, and the beam patterns for constant and variable (linearly-increasing) impedances. The calculated and experimental beam patterns are analyzed as a function of the length, the radius of the cylinder and the magnitude of the surface impedance.

Introduction

The use of antennas in the form of a cylindrical ribbed structure and a metallic cylinder with a dielectric layer as emitting systems is widely known. These systems, as well as a number of other antenna devices, belong to the class of emitters, on the surface of which boundary impedance conditions are fulfilled. Usually, the introduction of boundary impedance conditions makes it possible to comparatively simply determine the characteristics

of radiation of the antenna, obtained as a result of the solution of an external electrodynamic problem.

The method of solution of the electrodynamic problem is basically determined by the form of the given impedance surface. Thus, in the case of coincidence of the impedance surface with one of the coordinate surfaces of the coordinate system, in which the wave equation is separated according to the variable in [1], the method of eigen functions is used. In a number of cases, for example when the impedance surface is the surface of rotation [2], the problem is solved by the method of integral equations.

Given in the present study are the results of the application of the method of integral equations of the first order, with various areas of change of the observation and integration points [2], to the problem of determination of the characteristics of radiation of an impedance antenna in the form of a ribbed shaft, excited by a symmetrical dipole.

The problem of finding the magnitude of the impedance according to the given parameters of the antenna (depth and width of the channels of the ribbed structure, thickness and dielectric permeability of the dielectric layer on the metallic cylinder, and so on) [3], [4] or, conversely, calculation, according to the given magnitude of the surface impedance, of the parameters of the antenna, have independent interest, and are not examined here.

The coordinate systems utilized in this study are: rotation v, u, ϕ and cylindrical z, R, ϕ. The dependence on time is selected in the form $\exp(i\omega t)$.

Formulation and Method of Solution of the Problem. Current Distribution

Let there be an antenna in the form of an impedance body of

rotation, a specific case of which may be a cylinder of finite length. The antenna is excited by a symmetrical dipole, located perpendicular to its axis of rotation, with sinusoidal distribution of the volumetric density of the outside electrical current $\vec{j}^{\,\text{э.ст}}$ (Fig. 1). It is necessary to determine the radiation field of such an antenna.

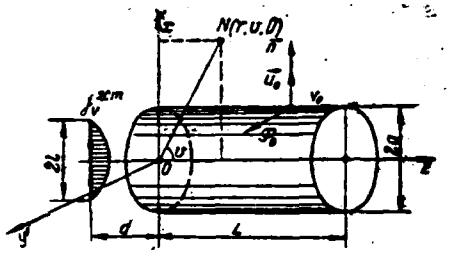

Fig. 1. Calculation of an impedance cylindrical antenna.

According to the theorem of equivalence, a complete field of radiation of an antenna is the sum of the primary and secondary fields, i.e.

$$\vec{E} = \vec{E}_{\text{перв}} + \vec{E}_{\text{втор}}, \tag{1}$$

where $\vec{E}_{\text{перв}}$ is the field created by the exciting outside sources (in the given case, the field of the exciting symmetrical dipole);

$\vec{E}_{\text{втор}}$ is the field created by the electrical and magnetic currents, excited on the surface of the impedance body.

Insofar as, on the surface of the body, the electrical and magnetic currents are associated through the boundary impedance condition, then, with a known impedance, it is sufficient to determine only one of these currents.

The system of two integral equations relative to the longitudinal $J^{\text{э}}_{\text{mv}}$ and lateral $J^{\text{э}}_{\text{m}\phi}$ components of the m harmonic of the surface density of the electrical current (more precisely, relative

to the coefficients of expansion of the desired current into a Fourier series according to the azimuthal coordinate), with selection of loop antennas with ϕ and z magnetic currents as auxiliary sources [2], after the switch to cylindrical coordinates, is written in the form:

$$\left.\begin{aligned}\int_v [K_1(v', v) J^s_{mv}(v) + M_1(v', v) J^s_{m\varphi}(v)] R dv = f_1(v')\\ \int_v [K_2(v', v) J^s_{mv}(v) + M_2(v', v) J^s_{m\varphi}(v)] R dv = f_2(v')\end{aligned}\right\}, \quad (2)$$

where

$$K_1(v', v) = \left\{\frac{iZ_1}{W_0}\left[\frac{\partial^2 S_m}{\partial R \partial R'} - \frac{\partial^2}{\partial z^2}\left(\frac{S_{m-1}+S_{m-1}}{2}\right) + \frac{\partial S_m}{\partial R'}\sin\Theta - \right.\right.$$
$$\left.\left. - \frac{\partial}{\partial z}\left(\frac{S_{m-1}+S_{m+1}}{2}\right)\cos\Theta\right\} R'; \quad (3)$$

$$M_1(v', v) = i\left\{\left\{\frac{\partial}{\partial z}\left(\frac{S_{m-1}-S_{m+1}}{2}\right) + \frac{iZ_2}{W_0}\left\{\frac{m}{R'}\frac{\partial S_m}{\partial z}\sin\Theta + \right.\right.\right. \quad (4)$$
$$\left.\left.\left. + \left[\frac{m}{R}\frac{\partial S_m}{\partial R'} - \frac{\partial^2}{\partial z^2}\left(\frac{S_{m-1}-S_{m+1}}{2}\right)\right]\cos\Theta\right\}\right\} R';$$

$$f_1(v') = -\frac{1}{k}\int_S \left\{\left\{\frac{1}{W_0}\left\{\frac{m}{R'}\frac{\partial S_m}{\partial z}\sin\Theta + \left[\frac{m}{R}\frac{\partial S_m}{\partial R'} - \right.\right.\right.$$
$$\left.\left. - \left[\frac{\partial^2}{\partial z^2}\left(\frac{S_{m-1}-S_{m+1}}{2}\right)\right]\cos\Theta\right\} j^{M.CT}_{mv} + \frac{i}{W_0}\left[\frac{\partial^2 S_m}{\partial R \partial R'} - \right.$$
$$\left. - \frac{\partial^2}{\partial z^2}\left(\frac{S_{m-1}+S_{m+1}}{2}\right)\right] j^{M.CT}_{m\varphi} + \left[\frac{\partial S_m}{\partial R'}\sin\Theta - \frac{\partial}{\partial z}\left(\frac{S_{m-1}+S_{m+1}}{2}\right)\right. \quad (5)$$
$$\left.\times\cos\Theta\right] j^{\ni.CT}_{mv} - i\frac{\partial}{\partial z}\left(\frac{S_{m-1}-S_{m-1}}{2}\right) j^{\ni.CT}_{m\varphi}\Big\} RR' ds; \quad (6)$$

$$K_2(v', v) = -\frac{im}{R}\left(S_m\cos\Theta + \frac{iZ_1}{W_0}\frac{\partial S_m}{\partial z}\right);$$

$$M_2(v', v) = \frac{\partial S_m}{\partial R} - \frac{iZ_2}{W_0}\left[\left(\frac{\partial^2 S_m}{\partial z^2} + S_m\right)\sin\Theta - \frac{\partial^2 S_m}{\partial R \partial z}\cos\Theta\right]; \quad (7)$$

$$f_2(v') = -\frac{1}{k}\int_S \left\{\frac{i}{W_0}\left[\left(\frac{\partial^2 S_m}{\partial z^2} + S_m\right)\sin\Theta - \frac{\partial^2 S_m}{\partial R \partial z}\cos\Theta\right] j^{M.CT}_{mv} + \right.$$
$$\left. + \frac{m}{W_0 R}\frac{\partial S_m}{\partial z} j^{M.CT}_{m\varphi} - \frac{im}{R} S_m\cos\Theta\, j^{\ni.CT}_{mv} + \frac{\partial S_m}{\partial R} j^{\ni.CT}_{m\varphi}\right\} Rds. \quad (8)$$

In these formulas, $Z_1 = E_v/H_\phi$ and $Z_2 = -E_\phi/H_v$ are the surface impedances, which are random functions of the longitudinal coordinate v, which do not depend on each other; R, z are the coordinates of the point on the surface of the excited body of rotation; R', z' are the coordinates of the point of location of the auxiliary sources; Θ is the angle between the direction of the vector of the normal $\vec{n}$ at the point v and the axis of rotation z; $W_0 = 120\pi$ ohms is the wave resistance of the free space. The linear dimensions in expressions (3)-(8), and below, are normed, i.e., they are multiplied by the wave number for the free space

$k=2\pi/\lambda$. In the right-hand portions of the equations, the integral starts along the surface S in the meridional plane, occupied by the outside electrical $\vec{j}^{\ni \cdot CT}$ and magnetic $\vec{j}^{M \cdot CT}$ currents after their expansion into a Fourier series according to ϕ. The function S_m [5] is the m coefficient of the expansion of the Green function for free space according to the azimuthal coordinate.

Used during the calculation of the kernels and the right-hand portions for computation of the function S_m, as well as the auxiliary function $S_m^I = \frac{1}{z-z'} \frac{\partial S_m}{\partial z}$, as a function of $v^2=RR'$ and $\rho_0=\sqrt{(z-z')^2+(R-R')^2}$, are either the expansion of these functions into a series according to the Hankel functions of the semi-integral index (with small v and large ρ_0), or expansions into a series according to hypergeometric functions (with large v and small ρ_0). The convenience of utilization for calculations of the indicated expansions consists of the fact that recurrent relationships are used during the calculation of the Hankel functions and the hypergeometric functions of high orders.

Equations (2)-(8) are written for the general case of excitation of an impedance body of rotation by outside longitudinal and lateral electrical and magnetic currents. In the case of excitation of a body of rotation by a short ($l \leq \lambda/4$) electrical dipole, located perpendicular to the axis of rotation, mainly the first harmonic is excited. With m=1 in the expressions for the kernels and the right-hand portions of the integral equations, using the functional relationships in study [5], one may switch from complex dependences with first and second derivatives to dependences on a total of only four functions: S_0, S_1, S_0^I, S_1^I. Then, the expressions for the kernels are written as:

$$K_1(v', v) = \frac{iZ_1}{W_0}\left[R'(S_0 + 2S_0') - \frac{1}{R}\rho_{z/2}^2 S_1'\right] - (S_1 + v^2 S_0' - R'^2 S_1')\sin\Theta - \frac{z-z'}{R}(S_1 + v^2 S_0')\cos\Theta; \quad (9)$$

$$M_1(v', v) = i\left\{\frac{z-z'}{R} S_1 + \frac{iZ_2}{W_0}\left[(z-z') S_1' \sin\Theta - \left(R' S_0' - \right.\right.\right.$$
$$\left.\left.\left. - \frac{(z-z')^2 + R'^2}{R} S_1'\right)\cos\Theta\right]\right\};$$

$$K_2(v', v) = -\frac{i}{R}\left[S_1 \cos\Theta + \frac{iZ_1}{W_0}(z-z') S_1'\right]; \quad (10)$$

$$M_2(v', v) = -\left(\frac{1}{R} S_1 + R' S_0' - R S_1'\right) + \frac{iZ_2}{W_0}\frac{1}{\gamma}\left\{\left\{(z-z') \times\right.\right. \quad (11)$$

$$\left[R' \beta^2 (S_0 + 3S_0') - R\alpha^2 S_1 - \left(\rho_{\pi/2}^2 \frac{\beta^2}{R} + 3R\alpha^2\right) S_1'\right]\cos\Theta +$$

$$+ \left[2\nu^2 (z-z')^2 (S_0 + 3S_0') + \left[(z-z')^2 \rho_{\pi/2}^2 - \gamma\right] S_1 - \right. \quad (12)$$

$$\left.\left. - \left[(z-z')^2 (R^2 + R'^2) + (R^2 - R'^2)^2\right] S_1'\right\} \sin\Theta\right\},$$

where $\alpha = \sqrt{(z-z')^2 + R^2 - R'^2}$; $\beta = \sqrt{(z-z')^2 - R^2 + R'^2}$; $\gamma = \rho_{\pi/2}^4 - 4\nu^4$.

The right-hand portions of expressions (5) and (8), with sinusoidal distribution of the outside current along the dipole, perpendicular to the z-axis, $j_V^{\text{ст}} = I_0 \sin(l-R)$ with an accuracy of up to the constant multiplier (placing $I_0/\pi = 1$), take on the following appearance:

$$f_1(v') = -\int_0^l (z-z')\left(S_1 + \nu^2 S_0'\right)\sin(l-R)\, dR, \quad (13)$$

$$f_2(v') = -\int_0^l S_1 \sin(l-R)\, dR. \quad (14)$$

Writing the integral equations in this form makes it possible to easily find their solution on an electronic computer. The method of solution of the integral equation consists of their reduction to a system of linear algebraic equations by means of approximation of the desired current by a piece-wise constant function [2].

The order of the system of algebraic equations is determined by the number of elementary intervals into which the length of the generatrix of the body of rotation v is divided. The length of the elementary intervals Δv is selected from the approximated condition of constancy of the desired current in the given interval. As a result, the integrals from the kernels of the integral equations, according to the elementary segments Δv, are coefficients

of the system of algebraic equations. Thus, the dependence of the matrix of the system of algebraic equations is fully determined by the appearance of the kernels of the integral equations.

With an optimal selection of the type of auxiliary sources and the place of their location [2], the matrices of the system of algebraic equations have a distinctly-pronounced diagonal nature. The determinant of this system has a large magnitude, which makes it possible to solve the system of algebraic equations with a high degree of accuracy [6]. This system of algebraic equations is solved by the method of inversion of the matrix.

Developed in order to find the distributions of the current, through which the beam patterns are determined, was an algorithm for solving integral equations, and programs were written for the computer. Based on the numerous calculations carried out, one may conclude that the examined method makes it possible to sufficiently rapidly, and with a high degree of accuracy, determine the characteristics of antennas in the form of impedance bodies of rotation.

Given in Fig. 2 are the results of calculation of the distribution of the surface of density of the electrical current $J^{э}=|J|\ e^{i\Psi}$ on the impedance cylinder with parameters: ka=1, kL=10.2. It is assumed during the calculation that the surface impedance of an inductive nature on the cylindrical portion of length L had a constant magnitude: $\tilde{Z}_1=Z_1/W_0=il$. (Here and elsewhere, it is further assumed that, throughout the length of the generatrix, $\tilde{Z}_2=0$, i.e., the anisotropic structure is examined.) The integral equations relative to the longitudinal $I^{э}_{1v}$ and lateral $I^{э}_{1\phi}$ components of the electrical current were reduced to a complex system of algebraic equations of the 40th order (the number of elementary intervals on the generatrix of the body was equal to 20). The length of the elementary intervals had values $\Delta v\approx 0.6$. The exciting dipole was located a distance from the end of the cylinder

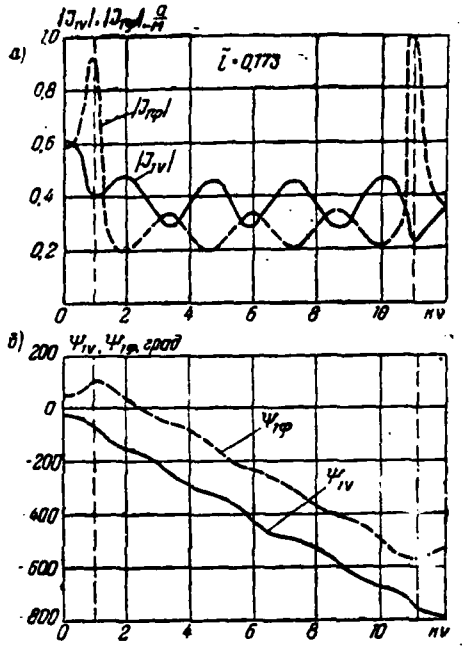

Fig. 2. Distribution of the amplitude (a) and phase (b) of the surface density of the electrical current on the cylinder with constant impedance (ka=1; kL=10.2; z_1=il).

kd=1.75, and had a length kl=1.5. For the amplitude of excitation of the dipole in expressions (13), (14), the coefficient of norming of the amplitude of the desired current $\tilde{I}$=0.173.

The presence of an appreciable reflected wave, brought about by the irregularity of the impedance at the point of change from the cylindrical portion of the surface to the end portion, is characteristic in the current distribution. It is evident from the distribution of the current phase that, as compared with an ideally-conducting cylinder, the current wave is slowed. At the point of change from the cylindrical portion of the surface to the end portion (it is assumed during the calculation that rounding of the radius kr_0=0.1 takes place at this point), a characteristic increase in the ϕ current, parallel to the edge, is noted.

For the case of a heterogeneous linearly-increasing impedance,

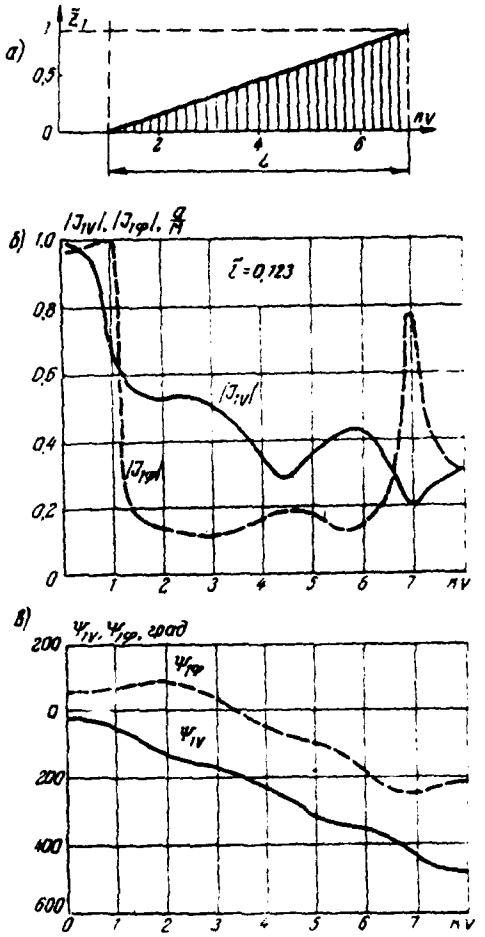

Fig. 3. Law of change in impedance (a) and distribution of amplitude (b) and phase (c) of the surface density of the electrical current on a cylinder of radius ka=1 and length kL=6.

the law of change of which along the generatrix of the cylinder is shown in Fig. 3a, the results of calculation of the current are presented in Fig. 3b, c. Here, in the current distribution, one may also note the presence of a wave reflected from the impedance drop. However, the amplitudes of the incident and reflected waves decrease along the surface more rapidly than on a cylinder with constant reactance, which is evidently brought about by the more intensive radiation because of irregularity of the impedance along

the surface of the cylinder.

Field of Radiation

As a result of the solution of the integral equations (2) for the problem of excitation of an impedance body of rotation, the harmonics of the surface density of the currents are found. The currents of the outside exciting sources are also represented in the form of an expansion according to harmonics. Therefore, it is also natural to find the field of radiation in the form of azimuthal harmonics, and to calculate the summary field as a Fourier series.

Written down in study [7] were the formulas for the m harmonics of the field of radiation from electrical longitudinal and lateral currents. The field of radiation from magnetic currents may be found in a similar manner through the corresponding vector potential. Utilized in this case is an asymptotic formula for the function S_m [5]:

$$S_m = i^m J_m(R\sin\vartheta)\, e^{iz\cos\vartheta}\,\frac{e^{-ir}}{r} \tag{15}$$

(where $J_m(x)$ is the Besselian function; R, z are the cylindrical coordinates of the discharge point; r, θ are the spherical coordinates of the observation point), as well as the functional relationships [8] for the Besselian functions of different index.

As a result, the general formula for the distribution of the surface density of the electrical $\vec{J}^{\ni}$ and magnetic $\vec{J}^{m}$ currents acquires the form:

$$E_{m\varphi}(r,\vartheta,\varphi) = e^{im\varphi}\frac{e^{-ir}}{2r} W_0 \int_v \Big\{ J^{\ni}_{mv}\, m\, i^{m-1}\cos\vartheta\,\frac{J_m(x)}{x} -$$
$$- J^{\ni}_{m\varphi}\Big[i^{m-1}\sin\Theta\sin\vartheta J_m(x) + i^m\cos\Theta\cos\vartheta\,\frac{dJ_m(x)}{dx}\Big] +$$
$$\frac{1}{W_0} J^{M}_{m\varphi}\, i^m\,\frac{dJ_m(x)}{dx} + \frac{1}{W_0} J^{M}_{mv}\, m\, i^{m-1}\cos\Theta\,\frac{J_m(x)}{x}\Big\} e^{iz\cos\vartheta} R\,dv; \tag{16}$$
$$E_{mz}(r,\vartheta,\varphi) = e^{im\varphi}\frac{e^{-ir}}{2r} W_0 \int_v \Big\{ J^{\ni}_{mv}\, m\, i^{m-1}\cos\Theta\,\frac{J_m(x)}{x} +$$

$$+J^{э}_{m\varphi}\, i^{m}\frac{dJ_m(x)}{dx}+\frac{1}{W_0}J^{м}_{m\varphi}\, m i^{m+1}\cos\vartheta\frac{J_m(x)}{x}-\frac{1}{W_0}J^{м}_{m\upsilon}\cdot$$
$$\times\left[i^{m+1}\sin\Theta\sin\vartheta J_m(x)+i^{m}\cos\Theta\cos\vartheta\frac{dJ_m(x)}{dx}\right]\Big\}e^{ix\cos\vartheta}Rd\upsilon. \qquad (17)$$

where $x=R\sin\theta$.

On the surface of an impedance body of rotation, the magnetic current is determined through the electrical current using the relationships:

$$J^{м}_{\varphi}=Z_1J^{э}_{\upsilon};\ J^{м}_{\upsilon}=-Z_2J^{э}_{\varphi}. \qquad (18)$$

It should be noted that formulas (16) and (17) determine both the amplitude (beam pattern) and phase characteristics of the field in the far zone, and are applicable for calculation of secondary and primary fields. For this, it is only necessary to integrate in the area occupied by the corresponding currents.

In the case, examined here, of excitation of only the first harmonic, formulas (16) and (17) are simplified:

$$E_{\vartheta}=A\int_{\upsilon}\Big\{\Big\{J^{э}_{1\upsilon}\Big\{-\sin\Theta\sin\vartheta J_1(x)+i\cos\Theta\cos\vartheta\Big[J_0(x)-$$
$$-\frac{J_1(x)}{x}\Big]\Big\}+J^{э}_{\varphi}\cos\vartheta\frac{J_1(x)}{x}+\frac{i}{W_0}J^{м}_{1\varphi}\Big[J_0(x)-\frac{J_1(x)}{x}\Big]+ \qquad (19)$$
$$+\frac{1}{W_0}J^{м}_{1\upsilon}\cos\Theta\frac{J_1(x)}{x}\Big\}\Big\}e^{ix\cos\vartheta}Rd\upsilon;$$
$$E_{\varphi}=A\int_{\upsilon}\Big\{\Big\{-J^{э}_{1\upsilon}\cos\Theta\frac{J_1(x)}{x}+J^{э}_{1\varphi}i\Big[J_0(x)-\frac{J_1(x)}{x}\Big]-$$
$$-\frac{1}{W_0}J^{м}_{1\varphi}\cos\vartheta\frac{J_1(x)}{x}+\frac{1}{W_0}J^{м}_{1\upsilon}\Big\{-\sin\Theta\sin\vartheta J_1(x)+ \qquad (20)$$
$$+i\cos\Theta\cos\vartheta\Big[J_0(x)-\frac{J_1(x)}{x}\Big]\Big\}\Big\}\Big\}e^{ix\cos\vartheta}Rd\upsilon.$$

where $A=W_0\dfrac{e^{-ir}}{2r}e^{i\phi}$ is the constant multiplier.

The design of the studied impedance antenna is shown in Fig. 4. During experimental verification, the surface impedance was determined through the structure parameters according to the well-known formula in [4]:

$$Z_1 = i W_0 \frac{t}{T} \left| \frac{J_1(ka) N_1(kb) - J_1(kb) N_1(ka)}{J_0(ka) N_1(kb) - N_0(ka) J_1(kb) - \frac{1}{ka} [J_1(ka) N_1(kb) - \right.$$

$$\left. - J_1(kb) N_1(ka)] \right|, \qquad (21)$$

where $N_0(x)$, $N_1(x)$ are the Neyman functions.

Presented in Figs. 5-8 are the experimental beam patterns, calculated according to formulas (19) and (20), with a change in the length and thickness of the antenna, and the magnitude of the homogeneous surface impedance, and examined in Fig. 9 is the case of heterogeneous impedance. In all of these figures, E_θ is the intensity of the entire electrical field in the plane zx, and E_ϕ is the intensity in the plane zy; the solid curve 1 is the calculated curve; the dot-and-dash curve 2 is the experimental curve; e is the norming coefficient.

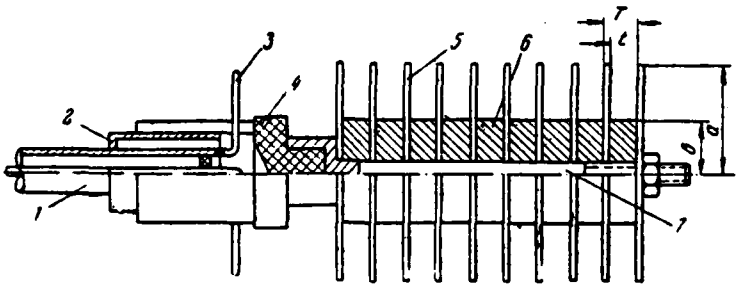

Fig. 4. Design of experimentally-studied antenna in the form of a ribbed shaft:
1 - coaxial line, 2 - four-wave cylinder, 3 - exciting dipole, 4 - insulator, 5 - disks, 6 - metallic inserts, 7 - central shaft.

It is evident from Figs. 5 and 6 that, with an increase in the length of the cylinder, the coefficient of directional action increases in the direction of the axis of the antenna ($\theta = 0$). In addition, an increase in the number of side interference lobes is characteristic, brought about by the nature of the change in amplitude of the current on the surface of the cylinder (see Fig.

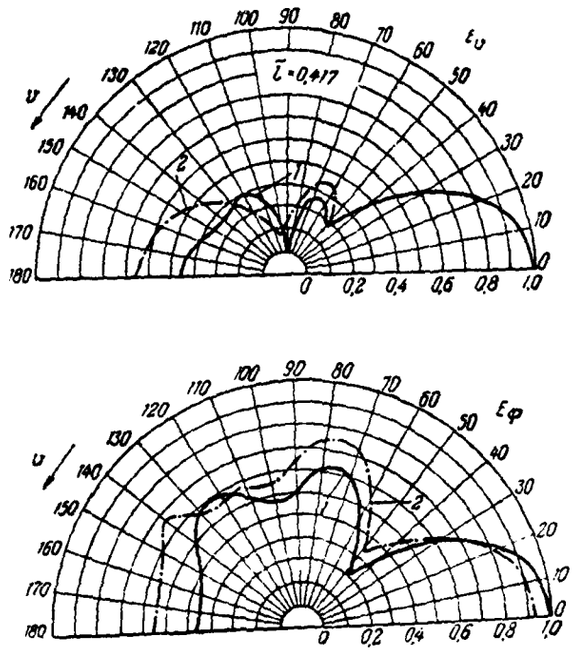

Fig. 5. Beam pattern of short cylinder with a constant inductive impedance (ka=1, kL=5, $\tilde{Z}_1$=i1).

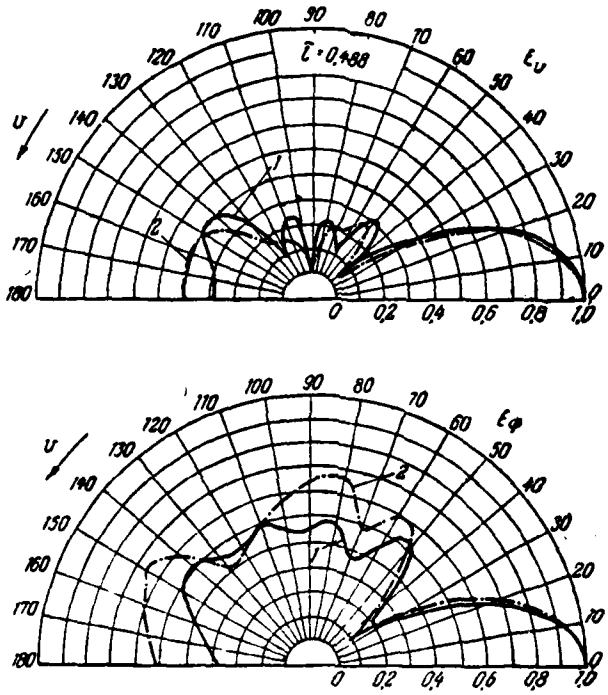

Fig. 6. Beam pattern of long cylinder with a constant inductive impedance (ka=1, kL=10.2, $\tilde{Z}_1$=i1).

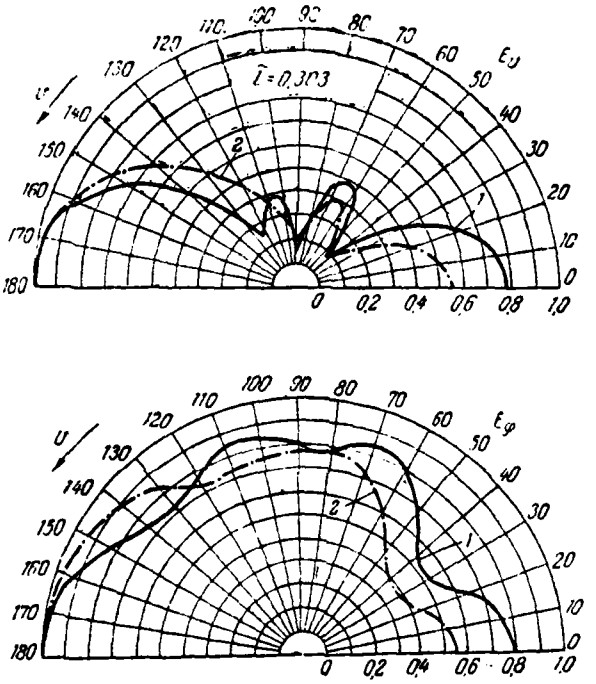

Fig. 7. Beam pattern of thick cylinder with small constant impedance (ka=1.6, kL=5.1, $\tilde{Z}_1$=i0.37).

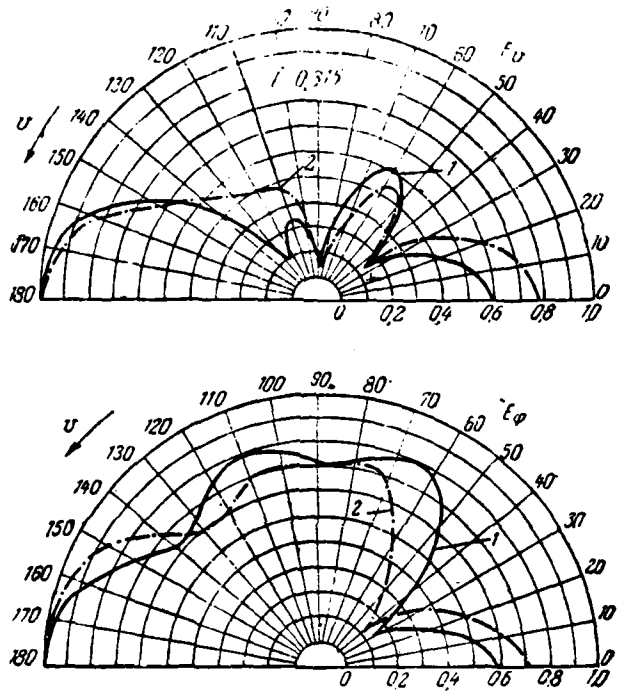

Fig. 8. Beam pattern of thick cylinder with increased surface impedance (ka=1.6, kL=5, $\tilde{Z}_1$=i0.74).

2). In the case of a thicker cylinder ka=1.6 (Figs. 7 and 8), as a result of the screening effect of the end portion and weaker excitation of the surface wave, the radiation in the inverse direction (θ=180°) turns out to be considerably greater. An increase in the magnitude of the surface impedance by twice leads to a less substantial change in the beam pattern than a change in length. For a cylinder with a linearly-increasing impedance (see Fig. 9), comparatively large radiation in the inverse direction is also noted, brought about by the wave reflected from the impedance drop on the right end of the cylinder.

During the conduct of the experiment, there is certain difficulty in obtaining the theoretical beam pattern of the symmetrical dipole (primary field) because of the presence of a coaxial feed cable and fastening elements, which introduce certain distortions into the radiation field. Naturally, this leads to a slight discrepancy in the calculated and experimental results.

In conclusion, we would note that, insofar as the problem of development of a specific antenna with given characteristics was not posed, we do not examine the question of optimization of the parameters of the ribbed-shaft structure and the appearance of the exciting source in the present article, which is completely possible in principle. The basic purpose is to show the possibility and the results of the application of the method of integral equations to the specific, practically interesting problem of the study of the characteristics of an antenna in the form of a ribbed shaft of finite length. The advantage of a similar approach to the solution of the problem consists of the sufficiently good approximation to a physically actual antenna (finiteness of length of the cylinder, shape, appearance of the exciting source) with a high degree of accuracy of calculation, brought about by the use of electronic computers.

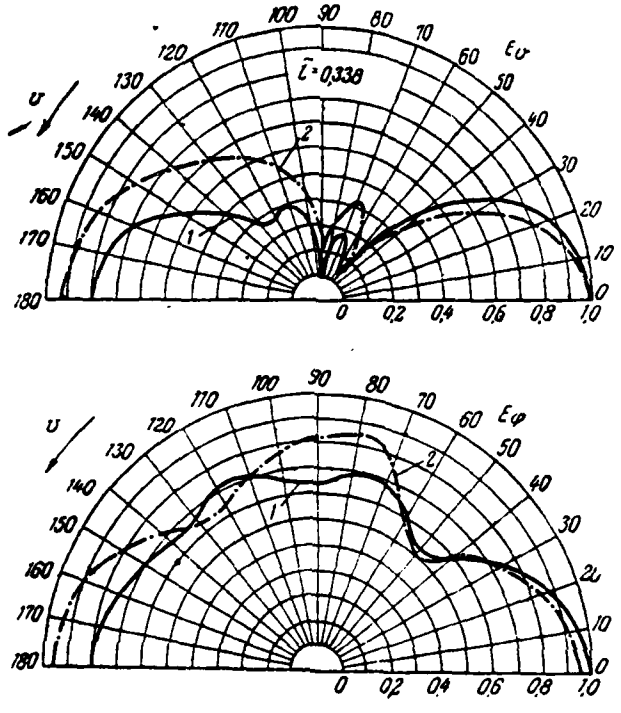

Fig. 9. Beam pattern of cylinder with linearly-increasing impedance.

Conclusion

Thus, we studied both theoretically and experimentally a cylindrical impedance antenna in the form of a ribbed shaft of finite length, excited by a symmetrical electrical dipole perpendicular to the axis of rotation and located on it. The current distribution on the surface of the antenna is found as a result of the numerical solution of integral equations of the first order, with various areas of change in the points of observation and integration. Also given are some results of the calculation of the distribution of the surface density of the electrical current for impedances which are constant and variable along the length of the shaft. General expressions are written down for determining the field of radiation of the harmonics of the electrical and magnetic currents. The calculated beam

patterns are also compared with the experimental beam patterns for various lengths and radii of the ribbed shaft with constant and variable (linearly-increasing) surface impedances.

The author expresses his gratitude to Ye. N. Vasil'ev for his direction in the present study.

ЛИТЕРАТУРА

1. Морс Ф. М., Фешбах Г. Методы теоретической физики, т. I. М. ИЛ 1958.
2. Васильев Е. Н., Малушков Г. Д., Фалунин А. А. Возбуждение импедансного тела вращения. «ЖТФ», т. 37, 1967, № 3, стр. 431.
3. Вайнштейн Л. А. Электромагнитные волны. М., изд. «Советское радио», 1957.
4. Фельд Я. Н., Бененсон Л. С. Антенно-фидерные устройства, ч. 2. М., 1959.
5. Васильев Е. Н. Об одной функции, встречающейся в теории дифракции, «ЖВМиМФ», т. 5, 1965, № 5, стр. 843.
6. Лаврентьев М. М. «Математический сборник», новая серия, т. 34 (76), 1954, вып. 1, № 2, 259.
7. Васильев Е. Н. Возбуждение гладкого идеально проводящего тела вращения. «Известия ВУЗов». Радиофизика, 2, 4, 1959, 588.
8. Янке Е., Эмде Ф. Таблицы функций с формулами и кривыми. М.-Л., ГИТТЛ, 1949.

POSSIBILITIES OF PHASE CORRECTION ON THE SMALL REFLECTOR IN A TWO-REFLECTOR ANTENNA

A. L. Ayzenberg

Analyzed in the approximations of geometric optics is the effect of redistribution of energy in a two-reflector system on the directive gain and noise temperature of the antenna with compensation of the phase errors, brought about by flexures of the basic (large) reflector, by means of automatic correction of the shape of the auxiliary (small) reflector. According to the results of the calculations, one may determine the maximum permissible deformations of the reflectors with given impairments of the antenna characteristics.

Introduction

In controlled reflector antennas of large diameters, it is difficult to ensure, and especially to maintain, the required precision of the reflector surface in the process of operation. In order to combat phase errors, which occur with weight, wind and temperature deformations of the basic reflector, a method was proposed for their automatic compensation by means of correction of the shape of the auxiliary (small) reflector in a two-reflector antenna [1]. The correction may be accomplished according to a program (according to the results of preliminary calculations or measurements of the deformations of the large mirror) or in a closed system of automatic regulation with feedback (where continuous

indication of phase errors and their compensation takes place). Utilized for indication of phase errors or deviations of the surface of the large reflector from the theoretical shape may be a phasometric system with modulation of the reflected signals [1], [2].

In multi-reflector antennas, the initial surfaces of the reflectors are calculated proceeding from the requirements for producing both a planar phase front and an optimal amplitude distribution of the field in the antenna aperture (including the level of irradiation of the edges of the reflectors) [3]. Repeated optimization of the phase-amplitude distribution of the field with deformations of the large reflector would require a certain change in the surfaces of the two auxiliary reflectors simultaneously (two degrees of freedom are required for regulation of the two field parameters). The compensation, examined here, of errors of the large reflector, by means of correction of the shape of the surface of only one small reflector, is therefore unavoidably accompanied by a change in the amplitude distribution of the field at the aperture, and the power radiated beyond the edge of the reflectors. The given study is devoted to analysis of the effect of the indicated changes on the directive gain and noise temperature of the antenna. As a result, we will determine the limitations on the magnitudes of the maximum deformations of the small and, accordingly, large reflectors, which will be permitted with the given impairments of the antenna parameters.

Initial Prerequisites

Since deformations of the large and small reflectors vary slightly, and the diameter of the latter is much less than the diameter of the former, correction of the shape of the small reflector has the major effect on the amplitude redistribution of the field, and changes in the surface of the large reflector may be disregarded for simplification of analysis. With small (comparatively with the diameters of the reflectors) deformations,

they may be considered directional perpendicular to the initial surfaces.

It is assumed that deformations of both the large and small reflectors have a smooth nature. This makes it possible to make use of the methods of geometrical optics during analysis. A certain surface of the small reflector, on which the correction is accomplished, corresponds to the given surface of the large reflector, if, in this case, the mutual position of the irradiator and the apexes of the reflectors are fixed. Also assumed is the absence of shifts of the irradiator and the center of the small reflector relative to the original axis of symmetry of the system, i.e., invariability of their position relative to the central (nondeformed) portion of the large reflector[1].

We will examine a system of reflectors of parabolic and confocal hyperbolic profiles, because of which the correspondence between the angles of irradiation and the coordinates of the initial and deformed reflectors will be determined by relatively simple relationships. Utilizing this correspondence, and the principle of conservation of energy in incident and reflected beam pencils, one may find the redistribution of energy in a two-reflector antenna with phasing on the small reflector. For concreteness we will examine some characteristic and practically important cases of weight deformations[2] of the reflectors, which, however, does not disrupt the generality of the results of the analysis.

---

[1]This may be achieved practically both by purely constructive measures, and by means of independent automatic correction of the position of the small reflector and the irradiator. These measures facilitate accurate sighting of the antenna beam and simplify the autophasing system.

[2]In antennas of large diameters, weight deformations are decisive with moderate wind speeds, if, in addition, measures are taken to reduce temperature deformations.

Phasing with Axiosymmetric Deformations

We will dwell on the case when flexures of the large reflector are axiosymmetric, directed outward, and increase monotonously from the center to the periphery (Fig. 1). Weight deformations have such a nature with orientation of the axis of the antenna towards the zenith ($\alpha=0$), and correction of the shape of the small reflector makes it possible to avoid original adjustment of the surface of the large reflector.

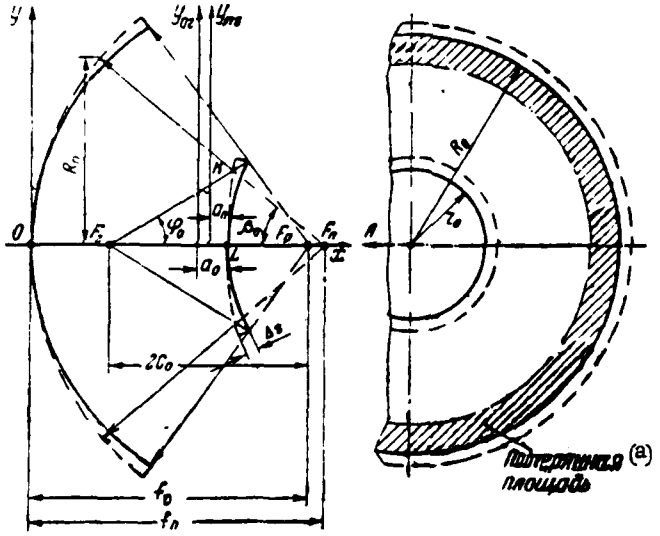

Fig. 1. Axiosymmetric deformations of the reflectors.
Key: (a) lost area

Assuming that the curve of flexure in the radial cross-sections is close to a quadratic parabola, one may assume that the deformed surface of the large reflector (paraboloid) is also a paraboloid, the apex of which coincides with the nominal apex (point 0) and the focal length f_n is greater than the initial focal length f_0. With correction, the small (hyperbolic) reflector, having straightened outwards, takes on the shape of a hyperboloid, the apex L and first focus f_1 of which remain the same as the initial, and the second focus coincides with the focus of the new paraboloid F_n (in Fig. 1,

the initial profiles of the reflectors are shown by the solid lines, and the deformed profiles by the dotted line).

We will examine the planar problem in the axial cross-section of the system. The initial parabolic and hyperbolic profiles in the inherent coordinate system x, y and x_0, y_0 are written:

$$y^2 = 4f_0x,$$

$$\frac{x_0^2}{a_0^2} - \frac{y_0^2}{c_0^2 - a_0^2} = 1.$$

where a_0, c_0 are the initial parameters of the hyperbola.

In this case,

$$x_0 = x - (f_0 - c_0),$$

$$y_0 = y.$$

The equations of the profiles of the deformed large and small reflectors in the inherent coordinate systems x, y and x_n, y_n have the form:

$$y^2 = 4f_nx, \tag{1}$$

$$\frac{x_n^2}{a_n^2} - \frac{y_n^2}{c_n^2 - a_n^2} = 1, \tag{2}$$

where

$$\left.\begin{aligned} x_n &= x_0 - (c_n - c_0) \\ y_n &= y_0 \end{aligned}\right\}, \tag{3}$$

$$f_n = f_0 + 2(c_n - c_0). \tag{4}$$

The new parameters of the hyperbola are

$$a_n = (c_0 + a_0) - c_n, \tag{5}$$

$$c_n = \frac{\sqrt{\left[(x_{0n} + c_0)^2 + y_{0n}^2\right]}(a + c_0) - (a_0 + c_0)^2}{\sqrt{(x_{0n} + c_0)^2 + y_{0n}^2} + x_{0n} + c_0 - 2(a_0 - c_0)}, \tag{6}$$

where x_{0n} and y_{0n} are the coordinates of the edge of the deformed hyperbola in the system x_0, y_0.

The latter are determined from the equalities:

$$\left.\begin{aligned} x_{0n} &= x_{00} + \Delta_r \eta_{x0} \\ y_{0n} &= y_{00} + \Delta_r \eta_{y0} \end{aligned}\right\}, \qquad (7)$$

where x_{00} and y_{00} are the coordinates of the edge of the initial hyperbola in the system x_0, y_0;

Δ_r is the displacement of the edge of the small reflector along the normal to the initial profile;

and

$$\left.\begin{aligned} \eta_{x_0} &= \mp \frac{x_{00}\left(c_0^2 - a_0^2\right)}{\sqrt{x_{00}^2\left(c_0^2 - a_0^2\right)^2 + y_{00}^2 a_0^4}} \\ \eta_{y_0} &= \mp \frac{y_{00} a_0^2}{\sqrt{x_{00}^2\left(c_0^2 - a_0^2\right)^2 + y_{00}^2 a_0^4}} \end{aligned}\right\} \qquad (8)$$

are the direction cosines of this normal.

The signs in expressions (8) are determined by the direction of deformation of the paraboloid (outward or inward). In the given examination, with η_{x0}, we will take only the "minus" sign into account, and with η_{y0}, only the "plus" sign.

We will return to the examination of the effect of deformation of the reflectors on the antenna characteristics.

Shown in Fig. 1 is the nature of changes in the trajectories of the extreme beams of the pattern of the irradiator. In the phasing process, the beam, having passed through the edge of the nondeformed reflectors earlier, is reflected from the point $k(x_{nk}, y_{nk})$ of the corrected hyperbolic profile, and intersects the parabolic reflector at some distance from its edge. Thus, the deformations of the small reflector outward lead to under-irradiation of the peripheral portion of the large reflector. The unirradiated surface of the initial antenna aperture has the shape of a ring (with practically prevailing levels of initial irradiation of the edges of the reflectors, the peripheral ring will be partially illuminated, but the level of irradiation, and, consequently, the

utilization of the surface are negligible here).

One may show that the radius of the new emitting aperture is

$$R_n = 2f_n \operatorname{tg}\left[\frac{\varphi_0}{2} + \operatorname{arc\,tg}\left(\frac{a_n^2}{c_n^2 - a_n^2}\,\frac{y_{nk}}{x_{nk}}\right)\right], \tag{9}$$

where ϕ_0 is half the angle of irradiation of the hyperbolic reflector;

$$y_{nk} = \frac{\operatorname{tg}\varphi_0\,(c_n^2 - a_n^2)}{c_n - a_n\sqrt{1+\operatorname{tg}^2\varphi_0}},$$

$$x_{nk} = \frac{y_{nk}}{\operatorname{tg}\varphi_0} - c_n$$

$$\operatorname{tg}\varphi_0 = \frac{y_{00}}{x_{00} + c_0}.$$

The relative decrease in the area of the aperture is

$$\frac{S_n}{S_0} = \left(\frac{R_n}{R_0}\right)^2.$$

Carried out as an example were calculations for an antenna with a diameter D=100 m, with the following initial geometric parameters:

focal length of the paraboloid $f_0 = 0.36\ D$;

diameter of the hyperboloid $d = 0.063D$;

angle of irradiation of the paraboloid $2\theta_0 = 140°$;

angle of irradiation of hyperboloid $2\phi_0 = 20°$.

Presented in Fig. 2 are the curves of the dependence of the relative decrease in the radius R_n/R_0 and the area of the aperture S_n/S_0 of the examined antenna on the maximum deformations Δ_Γ. It is evident from the indicated curves that, for example, with $\Delta_\Gamma = 120$ mm, $S_n/S_0 \approx 0.76$, i.e., the loss in area reaches 24%.

The relative drop in the directive gain of the antenna is

$$\frac{G_n}{G_0} = \frac{S_n}{S_0}\,\frac{\nu_n}{\nu_0}\,\frac{P_n}{P_0}.$$

where ν_0 and ν_n are the coefficients of the surface utilization of initial (radius R_0) and new (radius R_n) emitting apertures;

P_n/P_0 is the ratio of the powers of the irradiator, intercepted by the large reflector in the initial and autophased antennas.

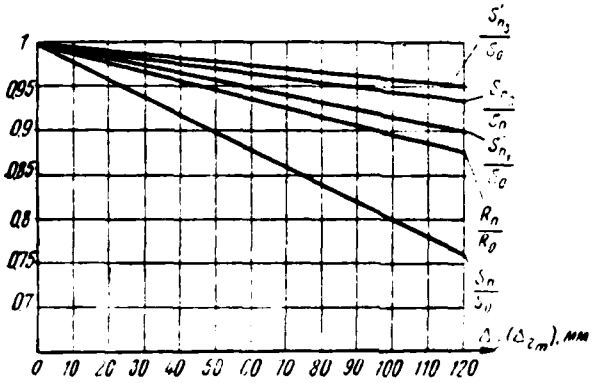

Fig. 2. Dependences of the relative decrease in radius and area of the antenna aperture on the maximum deformations of the small reflector.

The calculations for the case of quadratic flexures of the reflectors showed that the law of distribution of the field amplitude on the new aperture practically coincides with the distribution at the initial aperture, i.e., the coefficient of surface utilization of the emitting aperture is maintained unchanged in the phasing process ($\nu_n \approx \nu_0$). (This should be expected because of the fact that, with quadratic flexures, the change in the angles of inclination of the elementary sections of the small reflector occurs according to a linear law.) Since $P_n \approx P_0$, then the drop in the directive gain is determined by the reduction in the area of the aperture:

$$\frac{G_n}{G_0} \approx \frac{S_n}{S_0}.$$

With the examined deformations, the edges of the reflectors are irradiated at a lesser level than in the initial system, i.e., the noise temperature of the antenna is decreased slightly.

Phasing with Asymmetric Deformations

Asymmetric weight deformations (Fig. 3) are characteristic for an antenna oriented at some angle to the zenith: the flexures of the lower part of the large reflector are directed outwards, and the flexures of the upper part are directed inwards relative to the given surface. For the majority of designs, the deformations in the radial cross-sections increase according to a quadratic law from zero in the center to the maximum at the periphery of the reflector, while in circular cross-sections, they drop monotonously from maximum in the vertical axial plane to zero in the radial planes, oriented at angles Ψ to the equatorial plane.

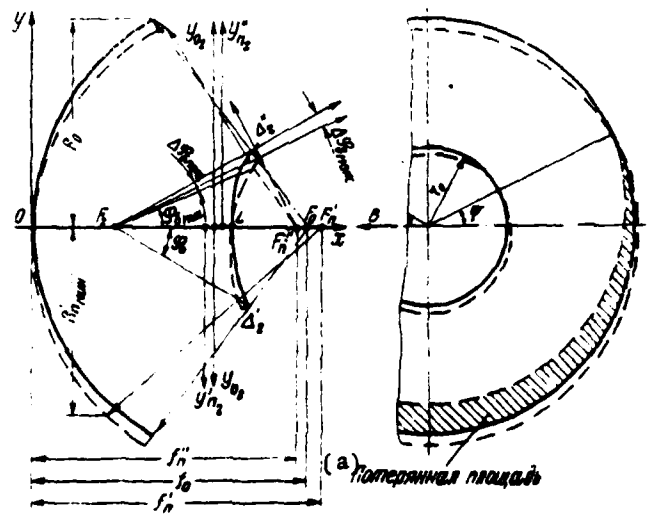

Fig. 3. Asymmetric deformations of reflectors.
Key: (a) lost area.

As a function of the method of initial phasing of the antenna (correction of the surface of the large or small reflector) and its design, the nondeformed radial profiles may lie below or above the equatorial plane ($\Psi<0$ or $\Psi>0$), and also coincide with it ($\Psi=0$). The lower and upper parts of the deformed surface of the

large reflector may be approximated by two sets of radial parabolic profiles, which have a general initial apex 0, and are determined, respectively, by the focal quarter-wave sections F_0F_n' and F_0F_n'', which lie along the original axis of symmetry of the system on both sides of the initial focus F_0. The focal length f_n vary between maximum values, which they take on in the vertical plane for the lower ($f_n'>f_0$) and upper ($f_n''<f_0$) parts of the reflector (the radial profiles, in which alternation of the sign of the flexures takes place, maintains the nominal focal length f_0).

During phasing, the hyperbolic reflector deforms so that the first focuses and the apexes of the radial hyperbolic profiles remain unchanged (points f_Γ and L), while the second focuses coincide with the focuses of the corresponding parabolic profiles.

The deformed radial parabolic and hyperbolic profiles of the lower and upper parts of the reflectors are determined as the functions of the deformations Δ_Γ' and Δ_Γ'' at the edges of the corresponding halves of the small reflector, using formulas (1), (4), (6), (7), (8) for the large reflector and (2), (3), (5), (6), (7), (8) for the small reflector. In expression (8) with η_{x0}, in this case, the "minus" sign is taken for the lower part of the reflector, and the "plus" sign is taken for the upper part, and vice versa with η_{y0}.

Correction of the shape of the lower part of the small reflector leads to partial under-irradiation of the large reflector [the lost surface of the initial aperture is a curvilinear segment (Fig. 3)]. The relative decrease in the area of the aperture is

$$\frac{S_n'}{S_0} \approx 1 - \frac{1}{4}\left(1 + \frac{2\psi}{\pi}\right)\frac{R_0^2 - R_{n\,\text{мин}}^2}{R_0 R_{n\,\text{мин}}}.$$

where the least radial dimension $R_{n\,\text{мин}}$ of the new emitting aperture is determined according to formula (9), with the substitution in it of the parameters of the lower vertical radial profiles of the

reflectors.

Shown in Fig. 2 are the dependences, calculated for a 100-meter antenna, of the reduction in area $\frac{S'_{n1}}{S_0}$, $\frac{S'_{n2}}{S_0}$ and $\frac{S'_{n3}}{S_0}$ (respectively for the cases $\Psi=\pi/4$, $\Psi=0$ and $\Psi=-\pi/8$) on the maximum deformations $\Delta'_{\Gamma m}$ of the lower edge of the small reflector. For example, with $\Delta'_{\Gamma m}$=120 mm, $\frac{S'_{n1}}{S_0}$=0.9, and $\frac{S'_{n3}}{S_0}$=0.95.

Correction of the shape of the upper part of the small reflector is accompanied by an increase in the level of irradiation of the upper edges of both reflectors, and an increase in radiation beyond their edges. We will evaluate the corresponding changes in the directive gain and noise temperature of the antenna.

The solid angle of the pattern of the irradiator (it is assumed that it is axiosymmetric), which includes the power $P_б$, lost beyond the edges of the large reflector, is:

$$\Delta\omega_б \simeq \frac{\pi}{2}\left(1-\frac{2\lambda}{\pi}\right)\left(\sin\frac{\varphi_{б\,мин}}{2}\operatorname{tg}\frac{\varphi_{б\,мин}}{4}-\sin\frac{\varphi_{б\,мин}-\Delta\varphi_{б\,макс}}{2}\right.$$
$$\left.\times\operatorname{tg}\frac{\varphi_{б\,мин}-\Delta\varphi_{б\,макс}}{4}\right),$$

where $\varphi_{б\ мин}$ is the minimum angle of the pattern of the irradiator, in which the energy intersects with the large reflector (Fig. 3);

$\Delta\varphi_{б\ макс}$ is the maximum "miss" angle wide of the large reflector.

The power $P_Г$, lost beyond the edges of the small reflector, is included in the solid angle:

$$\Delta\omega_г \simeq \frac{\pi}{2}\left(1-\frac{2\lambda}{\pi}\right)\left(\sin\frac{\varphi_0}{2}\operatorname{tg}\frac{\varphi_0}{4}-\sin\frac{\varphi_0-\Delta\varphi_{г\,макс}}{2}\operatorname{tg}\frac{\varphi_0-\Delta\varphi_{г\,макс}}{4}\right),$$

where $\Delta\varphi_{Г\ макс}$ is the maximum "miss" angle wide of the small reflector.

Given in Fig. 4 are the graphs, calculated for a 100-meter antenna, of the dependence of the "miss" angles $\Delta\varphi_б$ and $(\Delta\varphi_б+\Delta\varphi_Г)$

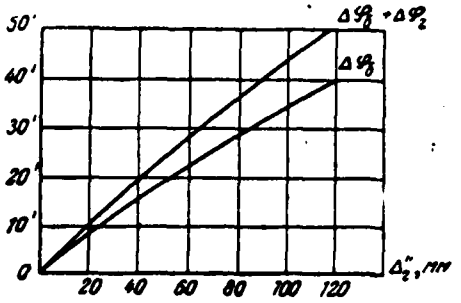

Fig. 4. Dependences of the "miss" angles $\Delta\phi_{\sigma}$ and $(\Delta\phi_{\sigma}+\Delta\phi_{\Gamma})$ on the deformation and Δ''_{Γ} with flexures of the large reflector inwards.

on the deformations Δ''_{Γ} at the edges of the upper part of the small reflector.

Shown in Fig. 5, for the case $\Psi=0$, are the curves of the dependence of the relative magnitudes of the solid angles $\frac{\Delta\omega_{\sigma}}{\omega_0}$ and $\frac{\Delta\omega_{\Gamma}+\Delta\omega_{\sigma}}{\omega_0}$ on the maximum deformations $\Delta''_{\Gamma m}$ of the upper edge of the small reflector (ω_0 is the solid angle of the pattern of the irradiator, in which the power P_0 is included).

The calculations, carried out on the basis of these graphs, showed that the relative power losses beyond the edges of the reflectors are insignificant. Thus, for $\Delta''_{\Gamma m}$=120 mm, they are 0.05% with initial irradiation of the edges of the reflectors at a zero level, and 0.5% with an initial level of the edge irradiation of 10 db. Thus, a reduction in the directive gain $\frac{G'_n}{G_0}$ in the case of asymmetric deformations is primarily determined by the decrease in the area of the aperture as a result of flexures of the lower part of the reflector:

$$\frac{G'_n}{G_0} \approx \frac{S'_n}{S_0}.$$

We will return to the noise temperature of the antenna.

An increase in the irradiation level, and, consequently, intensification of diffraction at the upper edges of the reflectors are small, as a result of the smallness of the angle $\Delta\phi_г$ and $\Delta\phi_б$, and, as the calculation showed, they are practically not reflected on the noise temperature of the antenna. Since

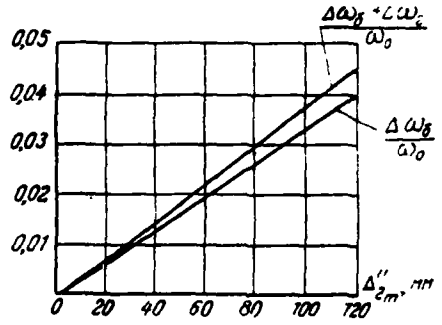

Fig. 5. Dependences of the relative magnitudes of the solid angles $\frac{\Delta\omega_б}{\omega_0}$ and $\frac{\Delta\omega_г+\Delta\omega_б}{\omega_0}$, which characterize the increase in radiation beyond the edges of the reflectors, on the deformations $\Delta''_г$.

$\Delta\phi_г \ll \Delta\phi_б$ and $\Delta\omega_г \ll \Delta\omega_б$ (Figs. 4 and 5), then $P_г \ll P_б$. In addition, the power $P_б$ is disseminated in the rear and distant side directions of radiation of the antenna, where a high temperature of the absorbing media is expected. Therefore, subsequently, we will take into account only the effect of the power $P_б$ which is predominant. In this case, the noise temperature of the autophased antenna is

$$T_a \simeq T_0 + \frac{P_б}{P_0}(T_б - T_0),$$

where T_0 is the temperature of the nondeformed antenna, and

$T_б$ is the temperature of the absorbing medium for the power $P_б$.

The temperature $T_б$ was determined by means of division of the solid angle $\Delta\omega_б$ into discrete sectors, and subsequent summation of the magnitudes of the noise from each sector [4].

Appreciable weight flexures of the large reflector inwards appear only with orientation of the antenna at some angle α to the zenith, and increase with an increase in this angle (the ratio of the powers P_σ/P_0 increases accordingly). At the same time, with an increase in α, the temperature T_σ decreases (since the portion of the power P_σ, directed at the "hot" earth and the high-temperature lower layers of the atmosphere decreases) and the temperature T_0 increases. Calculations for the case $\alpha=40°$ (with this angle, the flexures $\Delta''_{\Gamma m}$ may already reach substantial values, and the temperature difference $T_\sigma-T_0$ is greater yet) showed that the relationship of the portions of the solid angle $\Delta\omega_\sigma$, which correspond to radiation toward the earth, the lower layers of the atmosphere (up to 10° above the horizon) and the relatively "cold sky" (over 10° above the horizon) is 0.25:0.15:0.6. With study at the wave λ=3-5 cm, this corresponds to a temperature $T_\sigma \approx 100°K$. For $\alpha=40°$, the temperature of a well-designed antenna $T>20°K$. Examining, as an example, a 100-meter antenna for the case of maximum flexure of the small reflector $\Delta''_{\Gamma m}$=120 mm, and assuming that the average power level per unit of the solid angle $\Delta\omega_\sigma$ is 10 db lower as compared with the level in the angle ω_0, we have (see Fig. 5) $\frac{\Delta\omega_\sigma}{\omega_0}\approx 0.04$ and $\frac{P_\sigma}{P_0}\approx 0.004$, which corresponds to an increase in the antenna temperature by 0.3°K. Similar calculations for other angles α (with various values of Ψ) showed that the permissible deformations of the autophased antenna are primarily limited because of the reduction in the area of the aperture, while the relative increase in the antenna temperature is slight in this case.

The graphs in Figs. 2, 4 and 5, calculated for a 100-meter antenna, are suitable for antennas of random diameters with a proportional change in the magnitudes of the maximum deformation $\Delta_\Gamma(\Delta'_{\Gamma m})$.

With equal maximum deformations for the examined types of weight flexures, the greatest losses in area and reduction in

directive gain of the antenna accompany deformations of the axiosymmetric flexures. The indicated deformations are practically unequal. As a function of their relationship, determined by the design and the method of initial phasing of the antenna, the effect of both symmetric and asymmetric deformations may prove predominant.

The initial phasing of the antenna may be accomplished:

1) by means of correction of the surface of the small reflector;

2) by means of correction of the surface of the large reflector (i.e., elimination of axiosymmetric flexures with orientation of the axis of the antenna towards the zenith).

In the majority of designs, with asymmetrical deformations, in the former case, the angle $\Psi \geq 0$ (larger lower portion of the large reflector is deflected outward, and the smaller upper part is deflected inward), and in the latter case, $\Psi \leq 0$ (larger upper portion of the reflector is deflected inwards, smaller lower portion is deflected outwards). It is evident that with $\Psi > 0$, the deformations $\Delta'_{\Gamma m}$ are great, and the losses in area may reach considerable magnitudes (Fig. 2, curve $\frac{S'_{n1}}{S_0}$); here, the deformations $\Delta''_{\Gamma m} \leq \Delta'_{\Gamma m}$, and the increase in the antenna temperature because of a power overflow beyond the edges of the reflectors is negligible. With $\Psi < 0$, usually $\Delta'_{\Gamma m} < \Delta''_{\Gamma m}$ and, in addition $\Delta'_{\Gamma m}$ is less, and $\Delta''_{\Gamma m}$ is greater, as compared with the case $\Psi > 0$. Therefore, the losses in area are less here (Fig. 2, curve $\frac{S'_{n3}}{S_0}$), and we perceive that the increase in the antenna temperature is greater than with $\Psi > 0$. Nevertheless, in this case, as was already noted, limitations ensue, primarily because of the loss in area of the aperture.

Thus, during initial phasing of the antenna, both the axiosymmetric and, to a considerable extent, the asymmetric deformations of the reflectors are limited on the small reflector because of the loss in area. During initial phasing of the antenna, the

permissible deformations are increased considerably by means of elimination of axisymmetric flexures on the large reflector.

In the analysis given above, the changes in the characteristics of the antenna were determined as a function of flexures of the small reflector. The change to the corresponding flexures of the large reflector may be accomplished using formula (1). The connection between the small deviations $\Delta_г$ and $\Delta_б$ at the edges of the small and large reflectors may also be found according to the approximated formula:

$$\Delta_б \simeq \Delta_г \frac{\cos\frac{\beta_0+\varphi_0}{2}}{\cos\frac{\beta_0}{2}}.$$

With $2\beta_0=140°$ and $2\varphi_0=20°$, $\Delta_б \approx 0.94\Delta_г$.

The permissible deformations increase with an increase in the ratio of the diameters of the small and large reflectors.

It should be noted that the losses in area may be reduced by means of prescribing the initial amplitude distribution in the aperture and the level of irradiation of the edges of the reflectors of the nondeformed antenna with regard for subsequent energy redistributions during correction on the small reflector.

Conclusions

1. Compensation of phase errors of the antenna by means of correction of the shape of the small reflector is accompanied by appreciable losses in area of the aperture (as a result of under-irradiation of the peripheral part of the large reflector) and a reduction in the directive gain of the antenna. These losses determine the maximum deformations which may be permitted on the small and, accordingly on the large, reflectors of an autophased antenna.

2. During initial phasing of the antenna, [illegible]

AD-A107 321 FOREIGN TECHNOLOGY DIV WRIGHT-PATTERSON AFB OH F/G 9/5
ANTENNA (SELECTED ARTICLES),(U)
OCT 81 D M TRUSKANOV, A A PISTOL'KORS
UNCLASSIFIED FTD-ID(RS)T-0937-81 NL

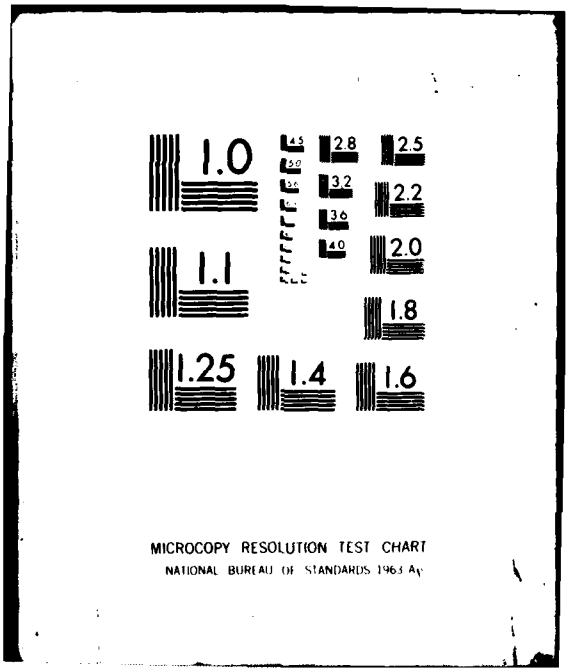
1.0
1.1
1.25
1.4
1.6
1.8
2.0
2.2
2.5
2.8
3.2
3.6
4.0
MICROCOPY RESOLUTION TEST CHART
NATIONAL BUREAU OF STANDARDS 1963 A

correction of the shape of the small reflector, the permissible deformations are considerably less than with elimination of the initial axiosymmetric flexures by means of correction of the surface of the large reflector.

3. With correction of the shape of the small reflector, which corresponds to flexures of the upper part of the large reflector inward, one may observe a slight increase in power overflow beyond the upper edges of the reflectors, and an increase in the level of their irradiation. This, however, reflects weakly on the noise temperature and directive gain of the antenna, even with considerable deformations.

4. The permissible deformations are proportional to the diameter of the antenna.

5. With the given antenna diameter, operation on shorter waves makes it possible to accomplish compensation of larger relative deformations, expressed in wave lengths.

In conclusion, the author expresses his sincere gratitude to L. N. Deryugin for direction of the study, and L. D. Bakhrakh, I. V. Vavilova, M. G. Kuznetsov and K. I. Mogil'nikova for their valuable advice and discussion of the results.

ЛИТЕРАТУРА

1. Айзенберг А. Л., Ардабьевский А. Н., Бахрах Л. Д., Дерюгин Л. Н., Кузнецов М. Г. Двухзеркальная антенна с автоматической компенсацией фазовых ошибок. Авт. свид. СССР № 170556 с приор. от 23/IV 1964 г., опубл. 12/V 1965 г. бюлл. № 9, стр. 36.
2. Айзенберг А. Л., Дерюгин Л. Н., Кузнецов М. Г. Двухзеркальная антенна с автоматическим фазированием и ее экспериментальное исследование. «Известия вузов МВ и ССО СССР». «Радиотехника», т. X, 1967, № 2, стр. 93.
3. Бахрах Л. Д., Могильникова К. И. Некоторые вопросы проектирования больших зеркальных радиотелескопов. «Известия вузов МВ и ССО СССР». «Радиофизика», т. 7, 1964, № 4, стр. 585.
4. Ditchfield C. R. Overall Sistem Requirements for Low Noise Performance. «British Inst. of Radio Eng.», august 1961, vol. 22, № 2, pp. 123–127.

END

DATE
FILMED

12-81
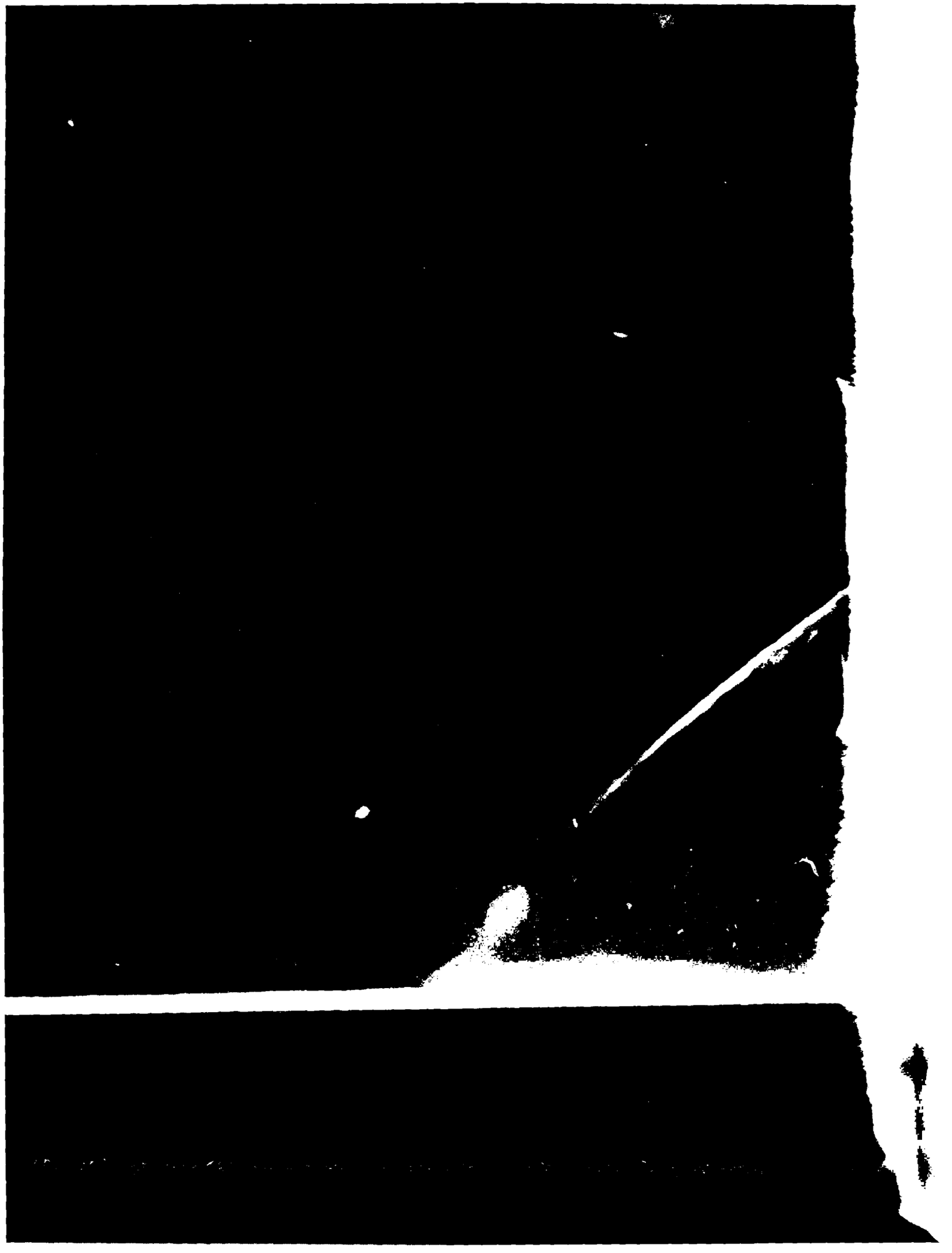
DTIC